Electronic Supplementary Information

Ultrahigh Power Generation from Low-Frequency and Micro Motion by Suppressing Air Breakdown

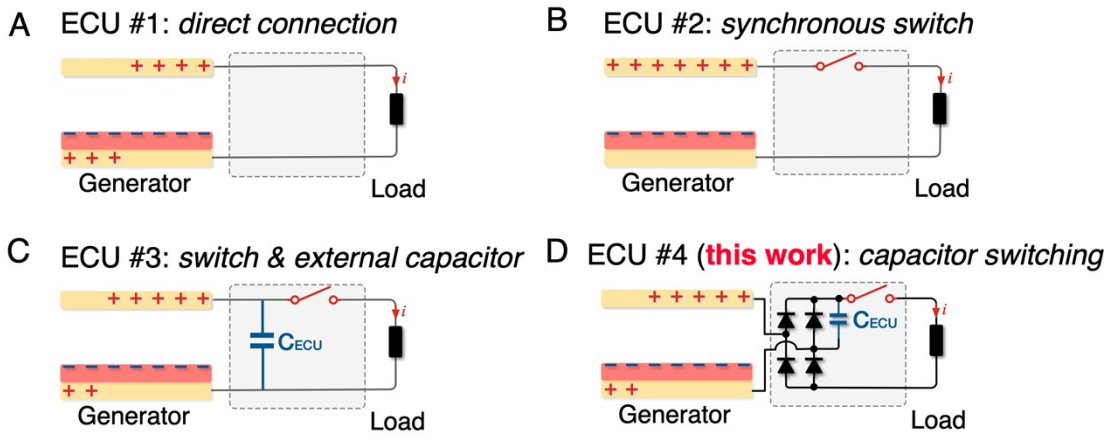

Figure S1. ECUs with different topologies.

(A) ECU #1: Direct connection, commonly referred to as the conventional generator.

(B) ECU #2: Synchronous switch.

(C) ECU #3: Synchronous switch with an external capacitor.

(D) ECU #4: Capacitor-switching (this work).

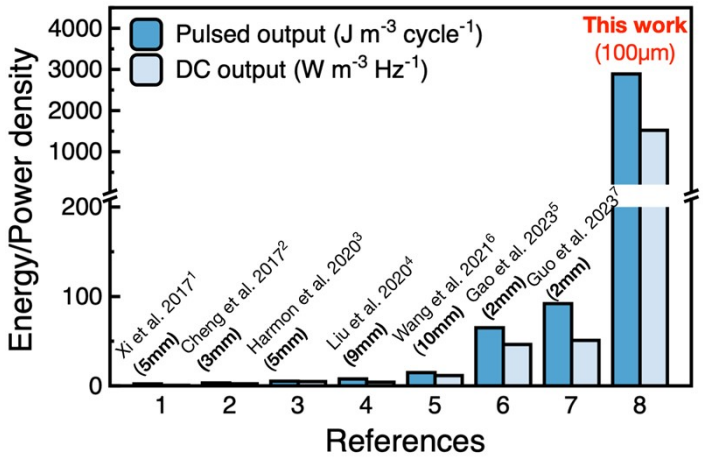

Figure S2. Output performance of this work compared with that in the latest and representative works (volumetric energy/power density).

The volume for the calculation of volumetric energy density refers to the difference between the maximum expansion volume and the compression volume of the generator.

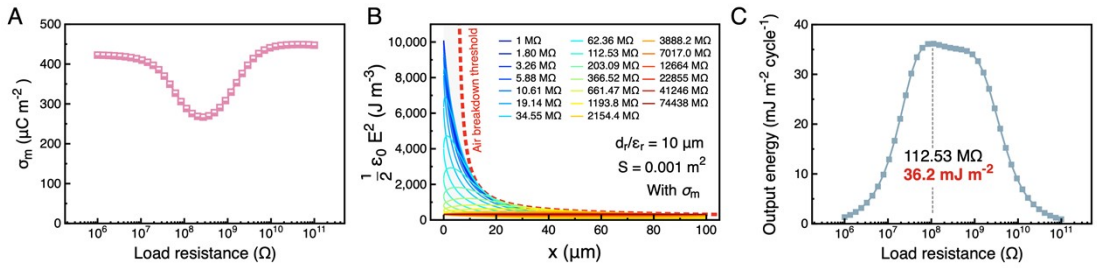

Figure S3. Maximum achievable output of the generator with ECU #1 (direct connection) under air breakdown limitation (d_r/ε_r = 10 μm, x_{max} = 100 μm, S = 0.001 m^2, sinusoidal excitation, 1 Hz).

(A) Maximum retainable charge density on the dielectric of the generator with different load resistances.

(B) Maximum achievable $\frac{1}{2}\varepsilon_0 E(x)^2 - x$ plots of the generator with different load resistances.

(C) Maximum achievable output energy of the generator with different load resistances.

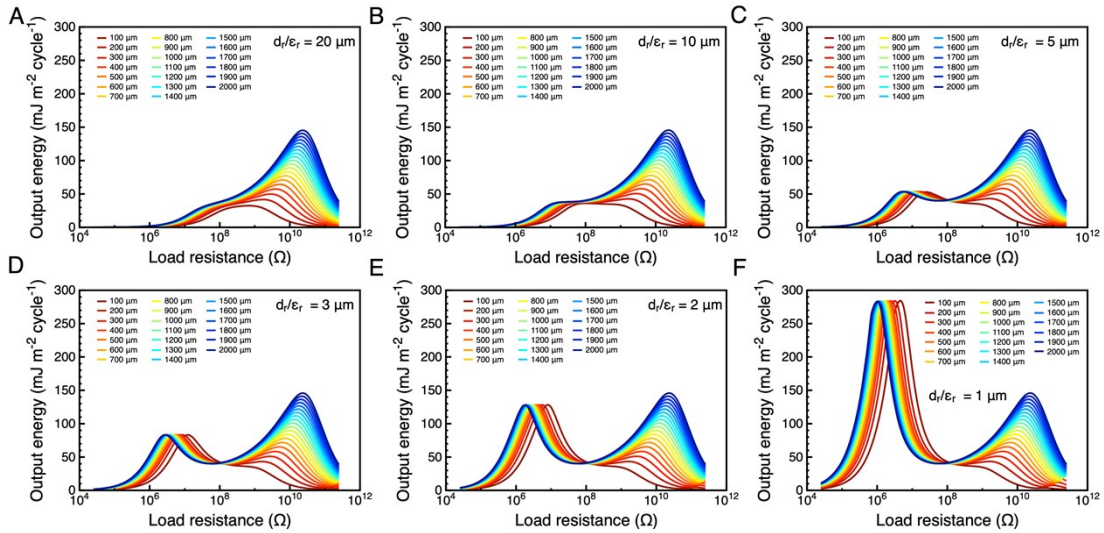

Figure S4. Maximum achievable output of the generator with ECU #1 (direct connection) under air breakdown limitation, considering different load resistances (R_L), different effective dielectric thicknesses (d_r/ε_r), and different maximum separation distances (x_{max}).

(S = 0.001 m^2, sinusoidal excitation, 1 Hz).

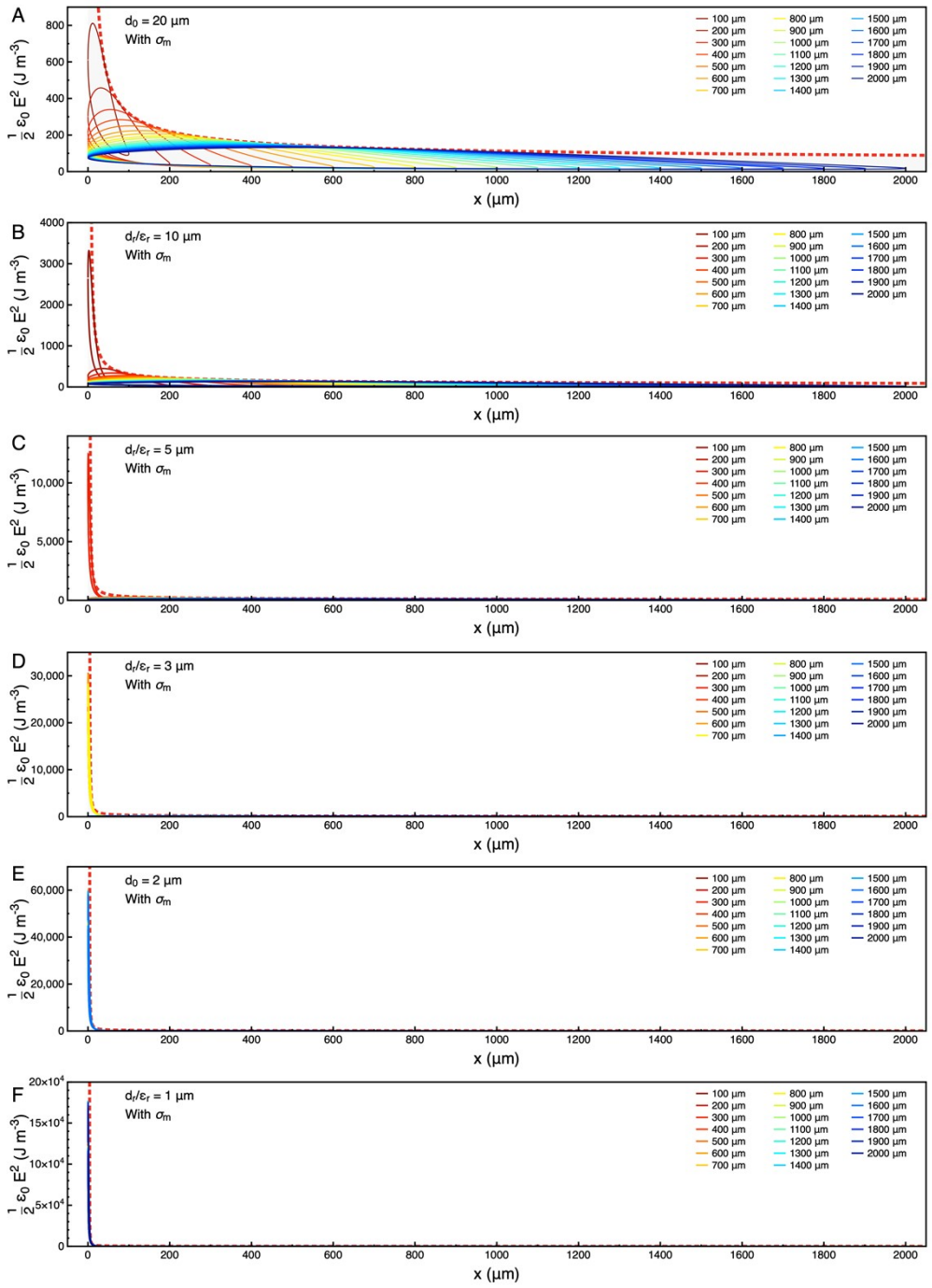

Figure S5. Maximum achievable $\frac{1}{2}\varepsilon_0 E(x)^2 - x$ plots of the generator with ECU #1 (direct connection) under air breakdown limitation, considering different effective dielectric thicknesses (d_r/ε_r) and various maximum separation distances(x_{max}). (With optimal load resistance, displayed in linear coordinates).

(S = 0.001m^2, sinusoidal excitation, 1Hz).

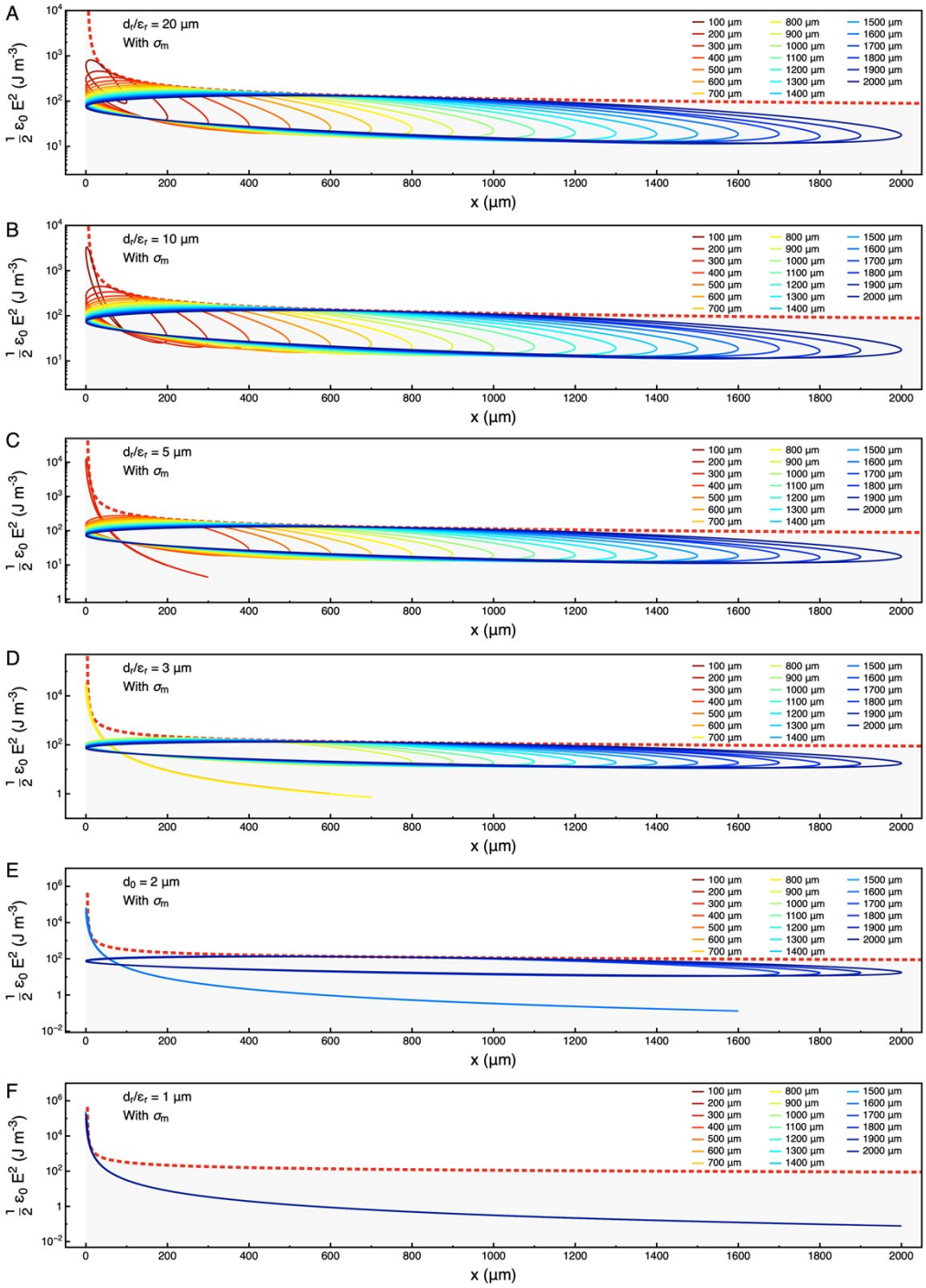

Figure S6. Maximum achievable $\frac{1}{2}\varepsilon_0 E(x)^2 - x$ plots of the generator with ECU #1 (direct connection) under air breakdown limitation, considering different effective dielectric thicknesses (d_r/ε_r) and various maximum separation distances (x_{max}). (With optimal load resistance, displayed in logarithmic coordinates).

(S = 0.001m^2, sinusoidal excitation, 1Hz).

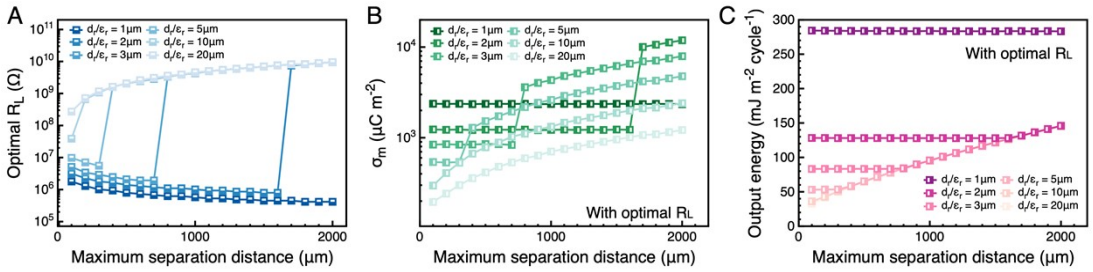

Figure S7. Maximum achievable output of the generator with ECU #1 (direct connection) under air breakdown limitation.

(A) Optimal load of the generator for maximizing the output.

(B) Corresponding maximum retainable charge density on the dielectric.

(C) Maximum achievable output energy of the generator.

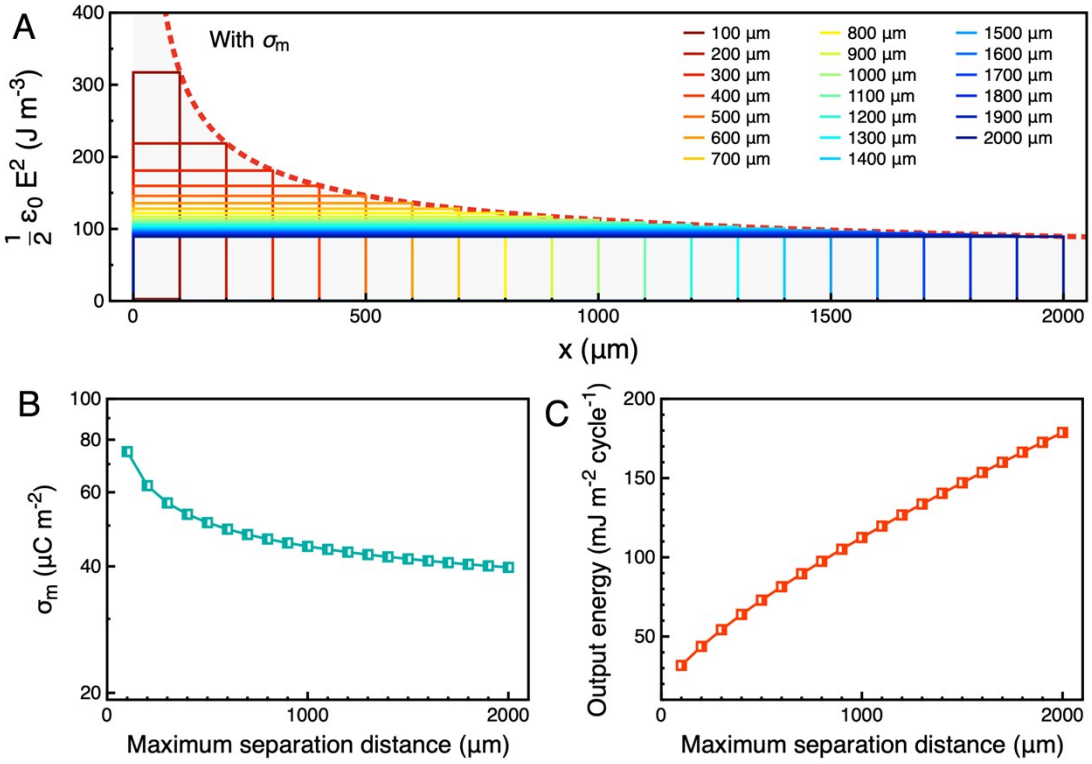

Figure S8. Maximum achievable output of the generator with ECU #2 (synchronous switch) under air breakdown limitation. The results are obtained under the assumption of that the load is sufficiently small.

(A) Maximum achievable $\frac{1}{2}\varepsilon_0 E(x)^2 - x$ plots of the generator.

(B) Corresponding maximum retainable surface charge density on the dielectric

(C) Maximum achievable output energy of the generator.

Note that the output of the generator with ECU #2 is independent of the thickness of the dielectric without considering the edge effects.

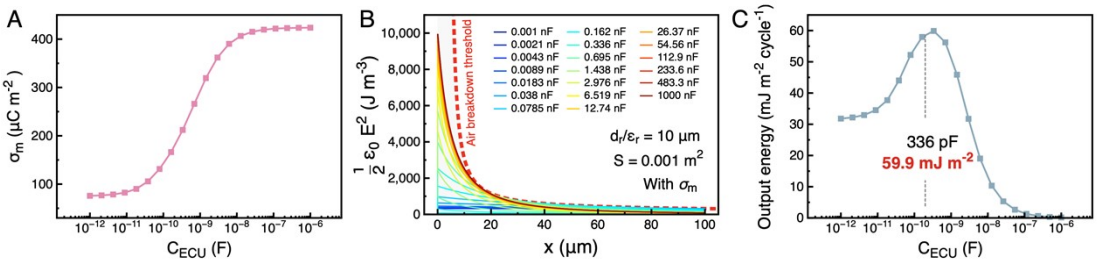

Figure S9. Maximum achievable output of the generator with ECU #3 (synchronous switch with an external capacitor) under air breakdown limitation (d_r/ε_r = 10 μm, x_{max} = 100 μm, S = 0.001m^2). The results are obtained under the assumption of that the load is sufficiently small.

(A) Maximum retainable charge density on the dielectric of generator with different external capacitances (C_{ECU}).

(B) Maximum achievable $\frac{1}{2}\varepsilon_0 E(x)^2 - x$ plots of the generator with different external capacitances (C_{ECU}).

(C) Maximum achievable output energy of the generator with different external capacitances (C_{ECU}).

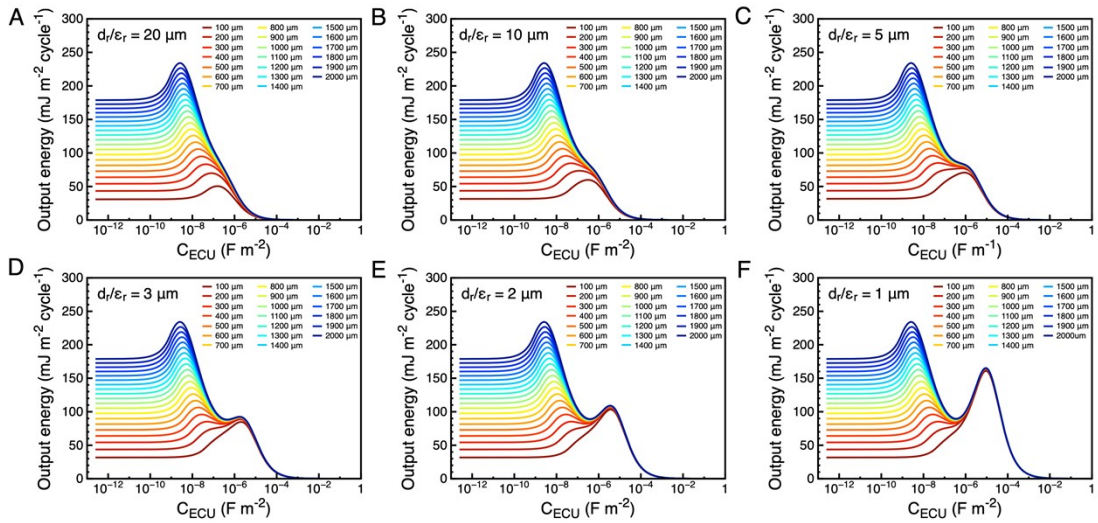

Figure S10. Maximum achievable output of the generator with ECU #3 (synchronous switch with an external capacitor) under air breakdown limitation, considering different external capacitances (C_{ECU}), different effective dielectric thicknesses (d_r/ε_r), and various maximum separation distances (x_{max}). The results are obtained under the assumption that the load is sufficiently small.

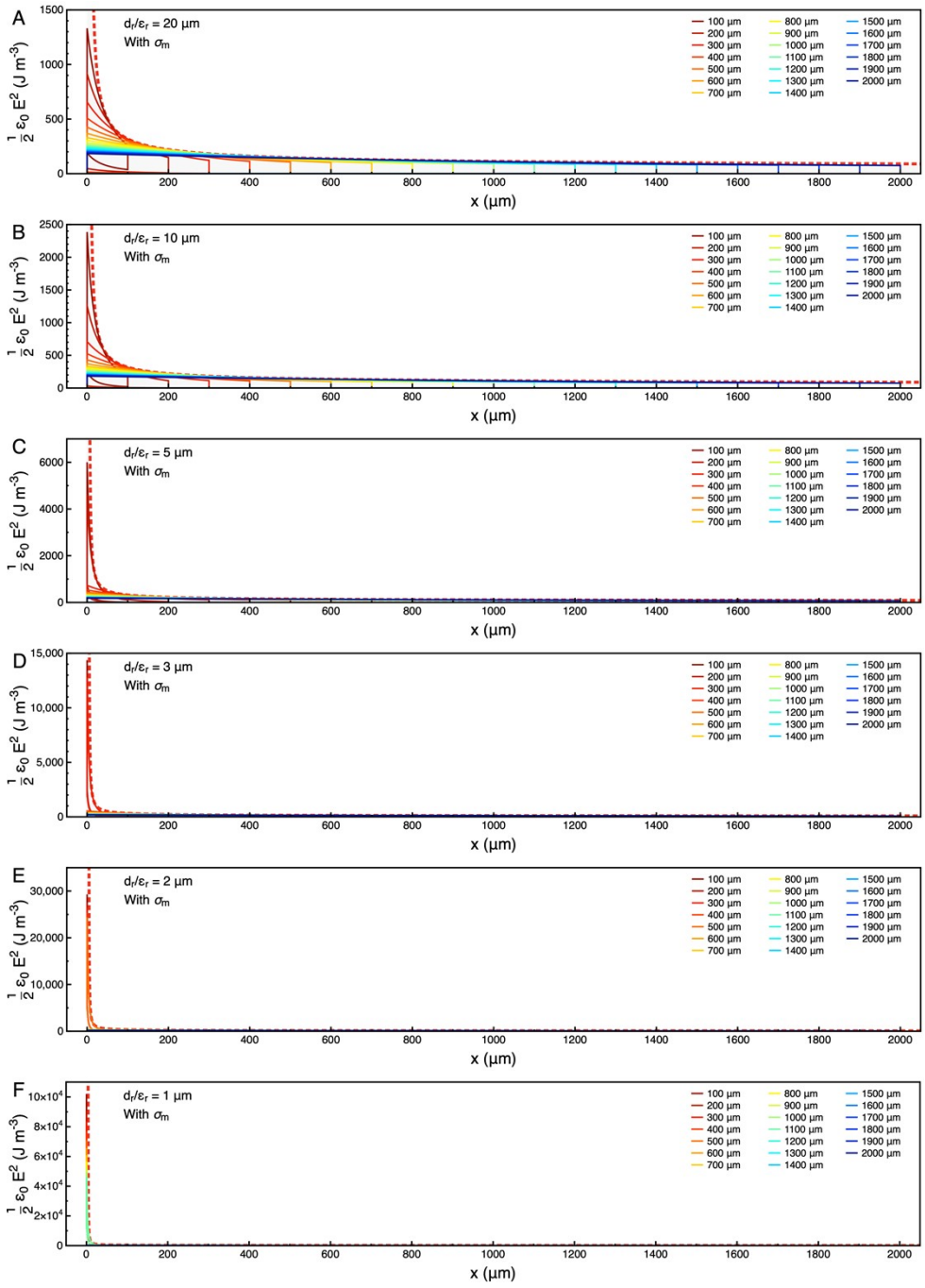

Figure S11. Maximum achievable $\frac{1}{2}\varepsilon_0 E(x)^2 - x$ plots of the generator with ECU #3 (synchronous switch with an external capacitor) under air breakdown limitation, considering different effective dielectric thicknesses (d_r/ε_r) and various maximum separation distances (x_{max}). (With optimal C_{ECU}, displayed in linear coordinates). The results are obtained under the assumption that the load is sufficiently small.

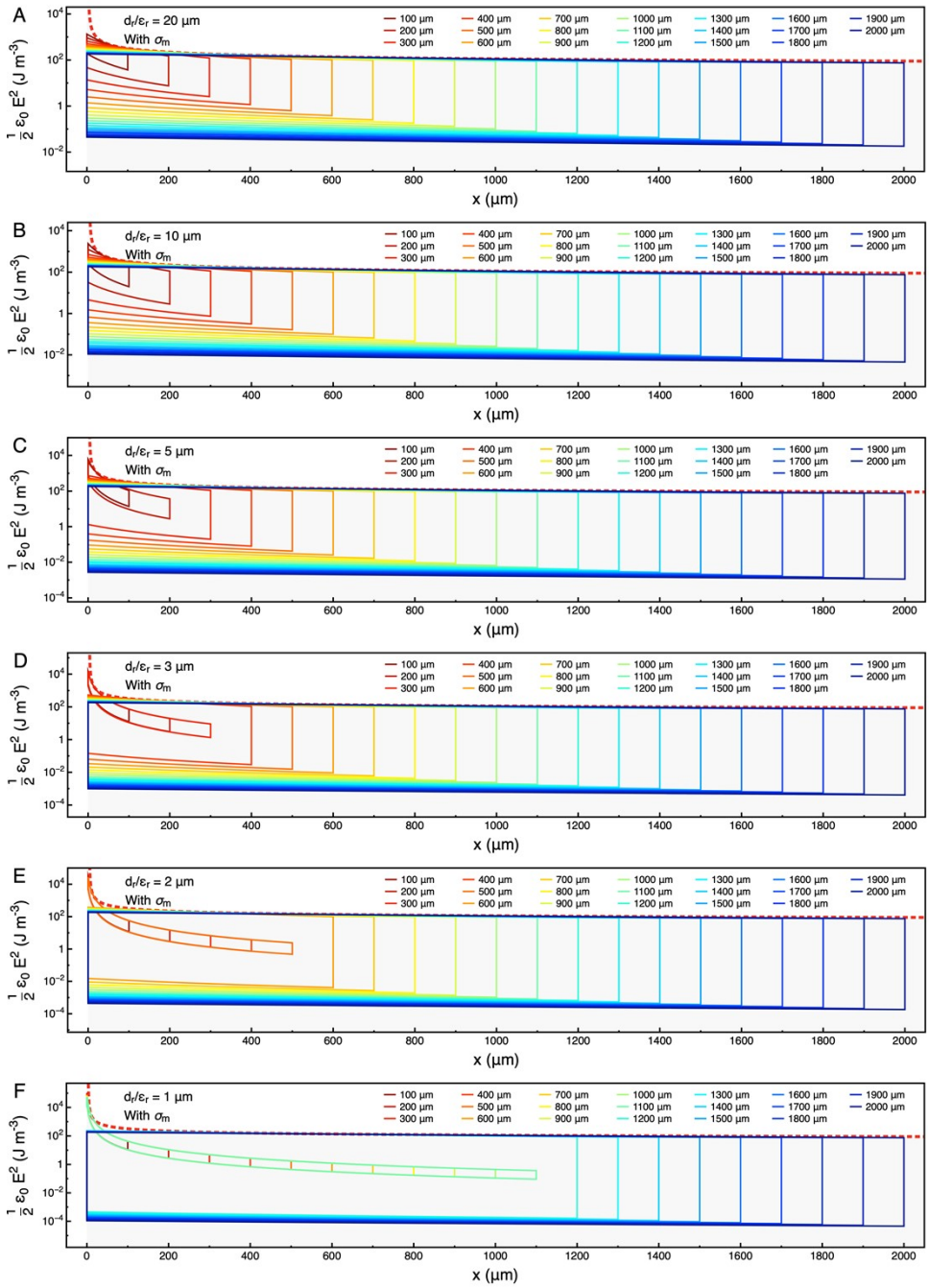

Figure S12. Maximum achievable $\frac{1}{2}\varepsilon_0 E(x)^2 - x$ plots of the generator with ECU #3 (synchronous switch with an external capacitor) under air breakdown limitation, considering different effective dielectric thicknesses (d_r/ε_r) and various maximum separation distances (x_{max}). (With optimal C_{ECU}, displayed in logarithmic coordinates). The results are obtained under the assumption that the load is sufficiently small.

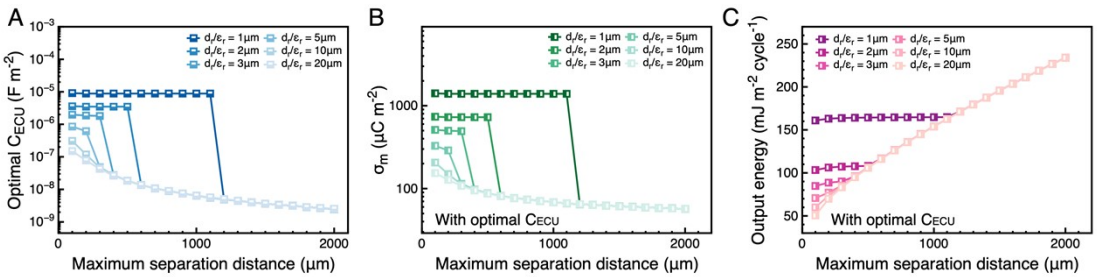

Figure S13. Maximum achievable output of the generator with ECU #3 (synchronous switch with an external capacitor) under air breakdown limitation. The results are obtained under the assumption that the load is sufficiently small.

(A) Optimal C_{ECU} of the generator for maximizing the output.

(B) Corresponding maximum retainable surface charge density on the dielectric.

(C) Maximum achievable output energy of the generator.

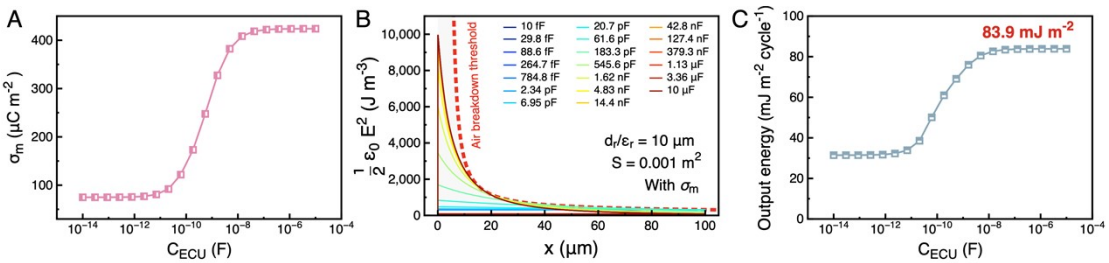

Figure S14. Maximum achievable output of the generator with ECU #4 (capacitor-switching) under air breakdown limitation (d_r/ε_r = 10 μm, x_{max} = 100 μm, S = 0.001 m^2). The results are obtained under the assumption that the load is sufficiently small.

(A) Maximum retainable charge density on the dielectric of generator with varying external capacitances (C_{ECU}).

(B) Maximum achievable $\frac{1}{2}\varepsilon_0 E(x)^2 - x$ plots of the generator with varying external capacitances (C_{ECU}).

(C) Maximum achievable output of the generator with varying load resistances with varying external capacitances (C_{ECU}).

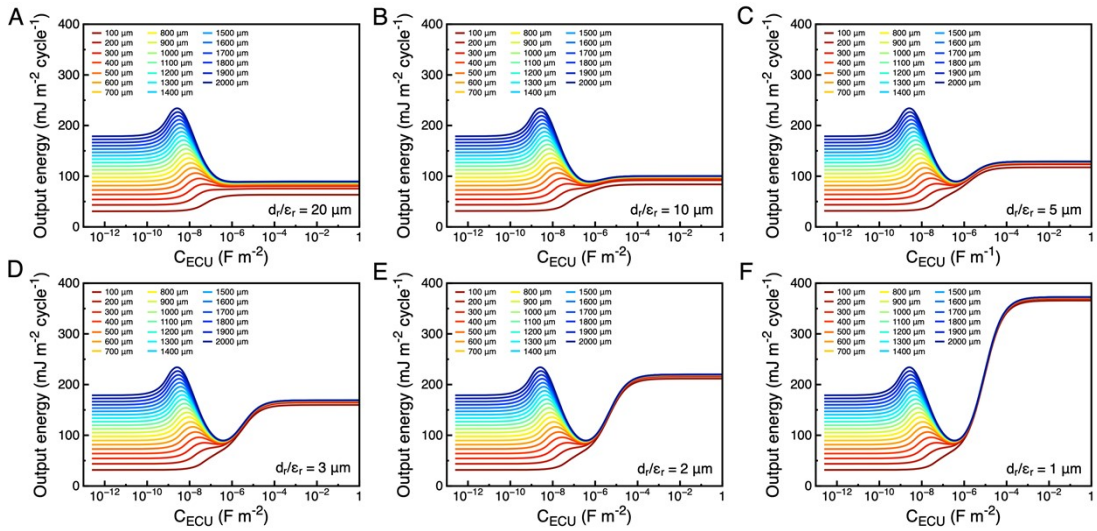

Figure S15. Maximum achievable output of the generator with ECU #4 (capacitor-switching) under air breakdown limitation, considering different external capacitances (C_{ECU}), different effective dielectric thicknesses (d_r/ε_r), and various maximum separation distances (x_{max}). The results are obtained under the assumption that the load is sufficiently small.

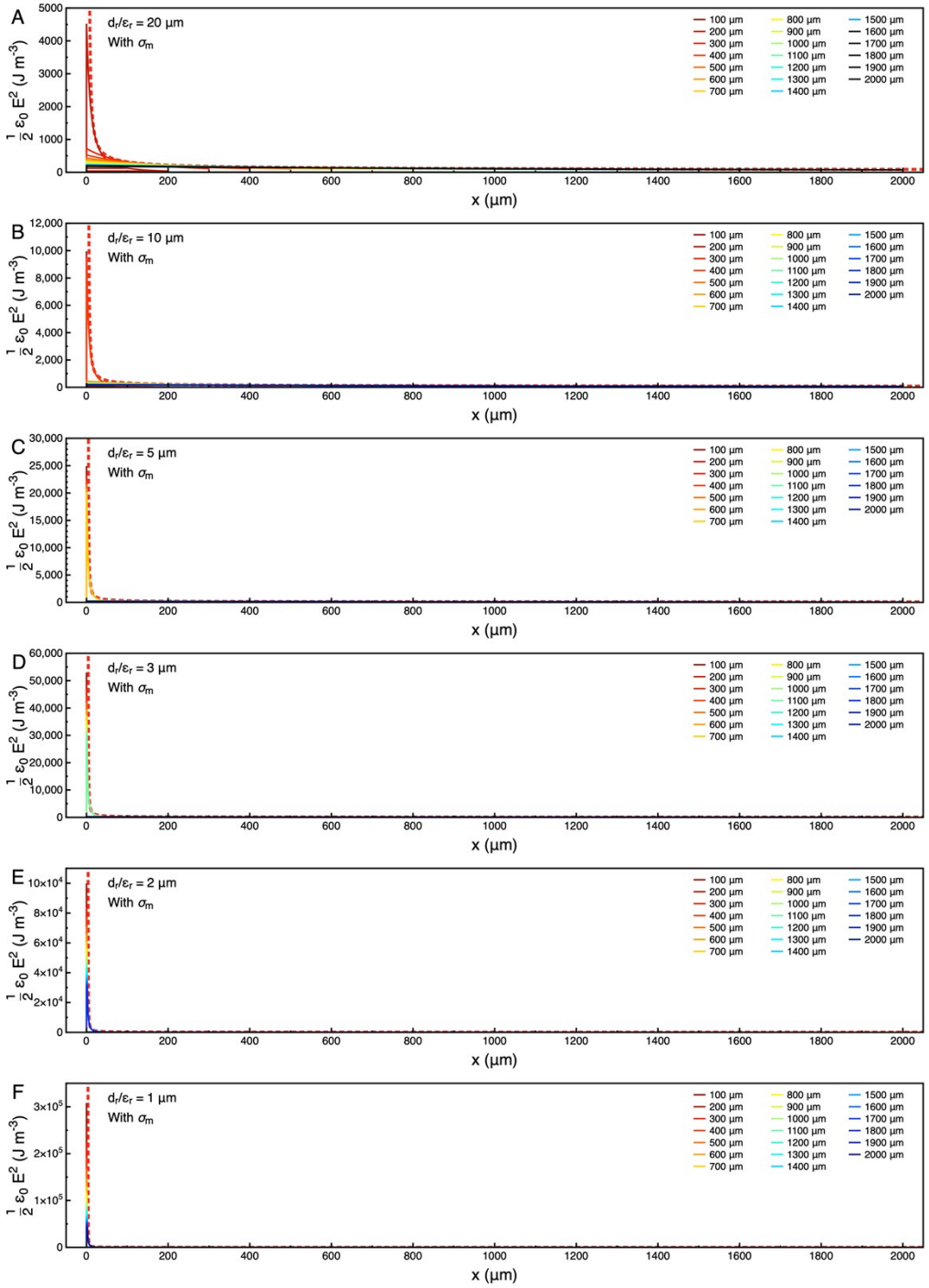

Figure S16. Maximum achievable $\frac{1}{2}\varepsilon_0 E(x)^2 - x$ plots of the generator with ECU #4 (capacitor-switching) under air breakdown limitation, considering different effective dielectric thicknesses (d_r/ε_r) and various maximum separation distances (x_{max}). (With optimal C_{ECU}, displayed in linear coordinates). The results are obtained under the assumption that the load is sufficiently small.

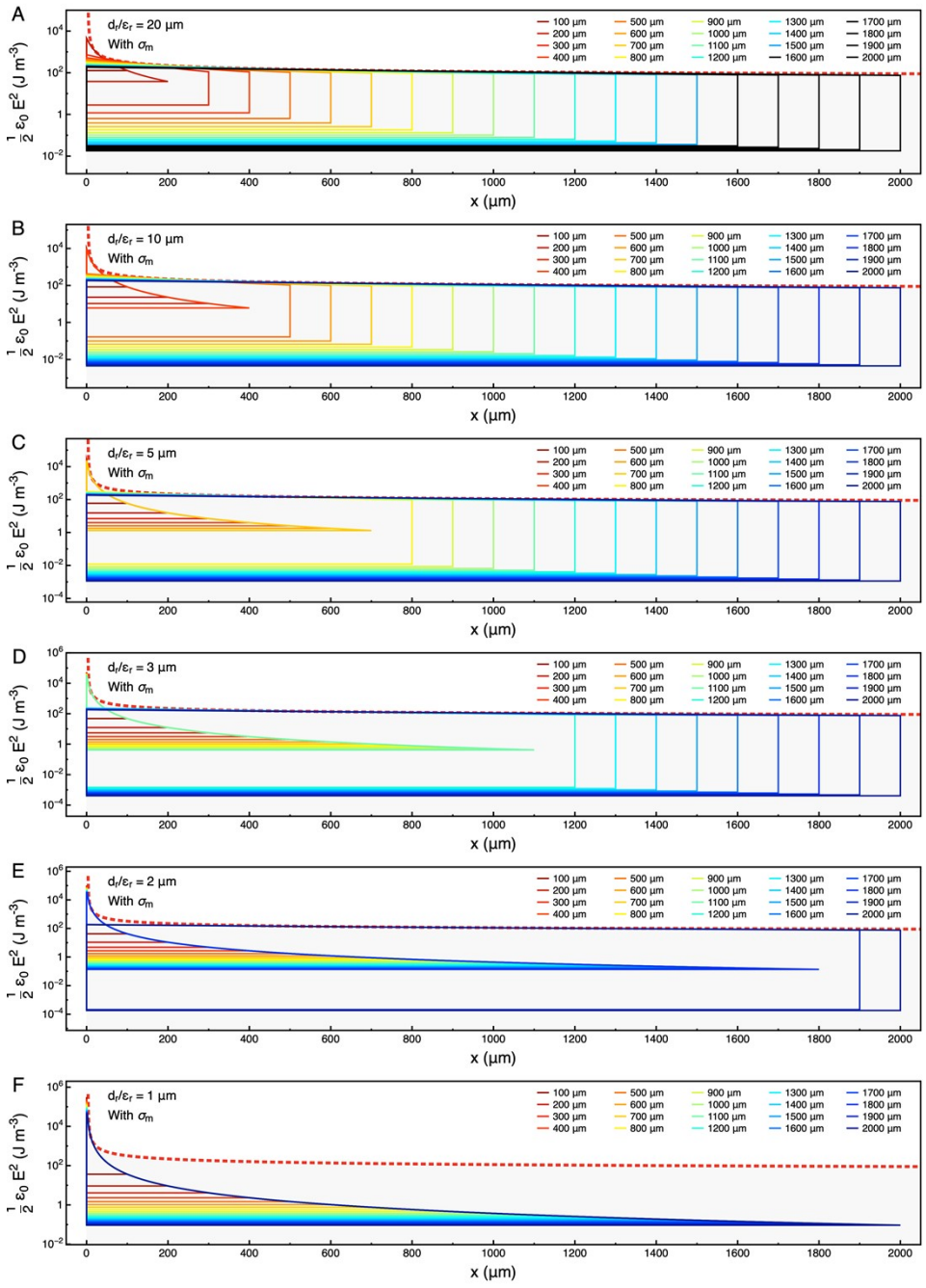

Figure S17. Maximum achievable $\frac{1}{2}\varepsilon_0 E(x)^2 - x$ plots of the generator with ECU #4 (capacitor-switching) under air breakdown limitation, considering different effective dielectric thicknesses (d_r/ε_r) and various maximum separation distances (x_{max}). (With optimal C_{ECU}, displayed in logarithmic coordinates). The results are obtained under the assumption that the load is sufficiently small.

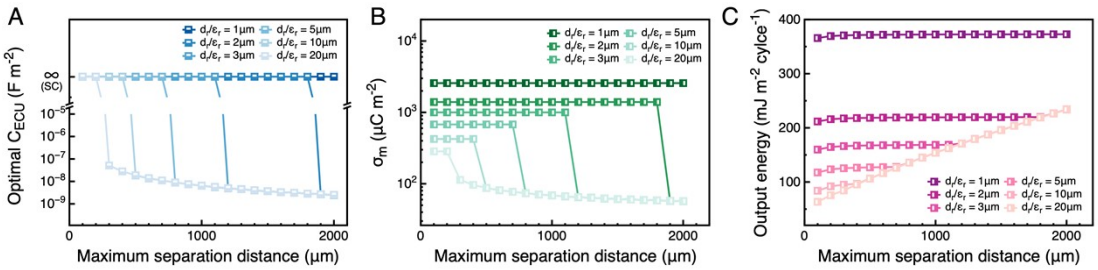

Figure S18. Maximum achievable output of the generator with ECU #4 (capacitor-switching) under air breakdown limitation. The results are obtained under the assumption that the load is sufficiently small.

(A) Optimal C_{ECU} of the generator for maximizing the output.

(B) Corresponding maximum retainable surface charge density on the dielectric.

(C) Maximum achievable output energy of the generator.

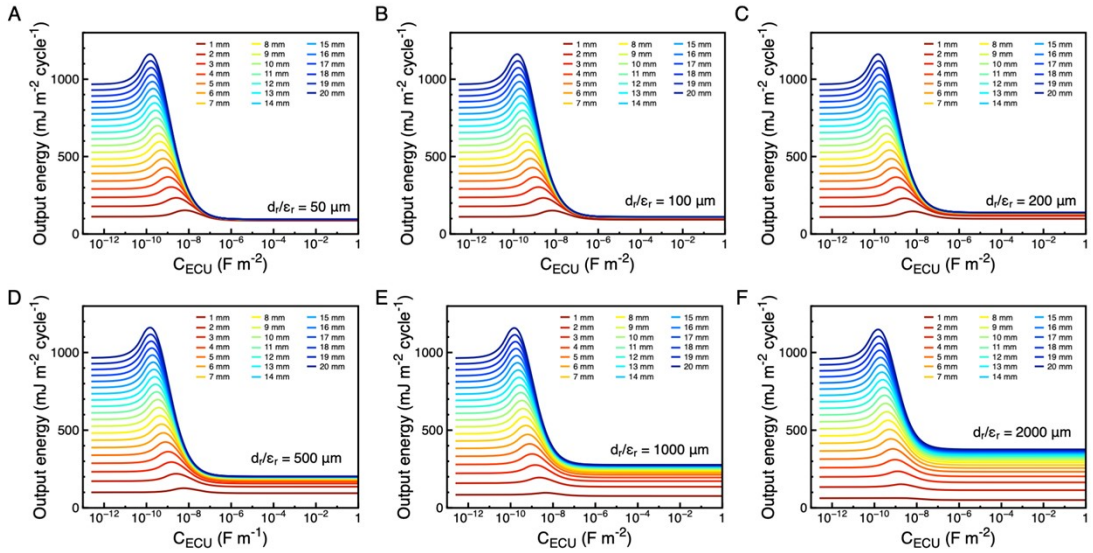

Figure S19. Maximum achievable output of the generator with ECU #4 (capacitor-switching) under air breakdown limitation, considering different external capacitances (CECU), different effective dielectric thicknesses (dr/εr), and various maximum separation distances (xmax). The results are obtained without considering the edge effects and under the assumption that the load is sufficiently small. (For larger dielectric thickness and separation distances)

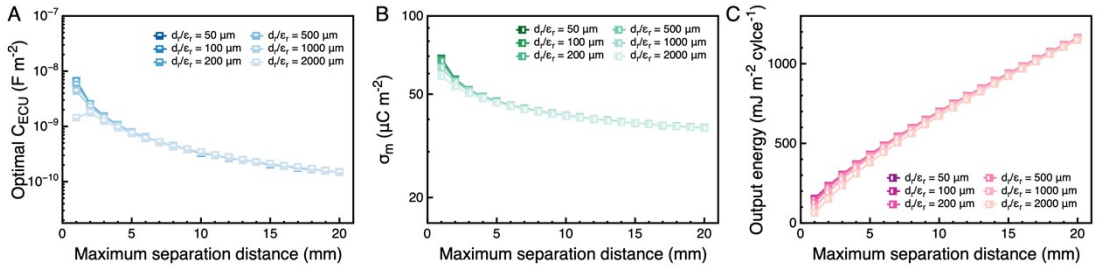

Figure S20. Maximum achievable output of the generator with ECU #4 (capacitor-switching) under air breakdown limitation. The results are obtained under the assumption that the load is sufficiently small. (For larger dielectric thickness and separation distances)

(A) Optimal CECU of the generator for maximizing the output.

(B) Corresponding maximum retainable surface charge density on the dielectric.

(C) Maximum achievable output energy of the generator.

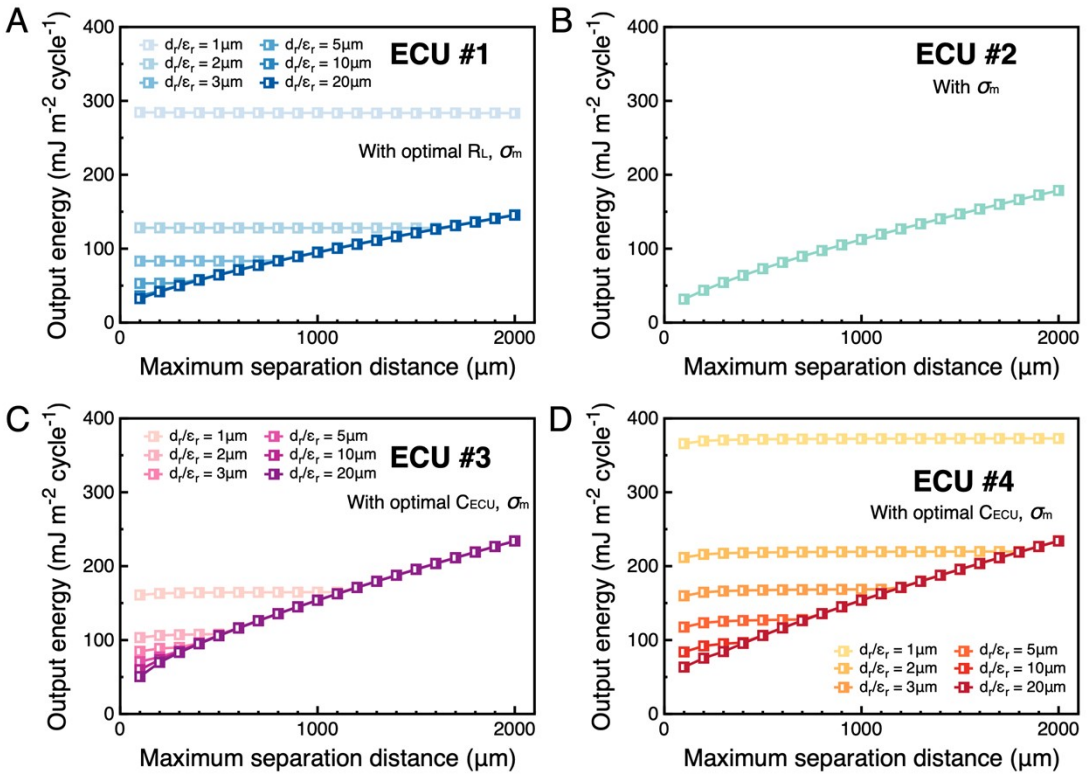

Figure S21. Comparison of the maximum achievable output of the generator with various ECUs.

(A) ECU #1: Direct connection, commonly referred to as the conventional generator.

(B) ECU #2: Synchronous switch.

(C) ECU #3: Synchronous switch with an external capacitor.

(D) ECU #4: Capacitor-switching (this work).

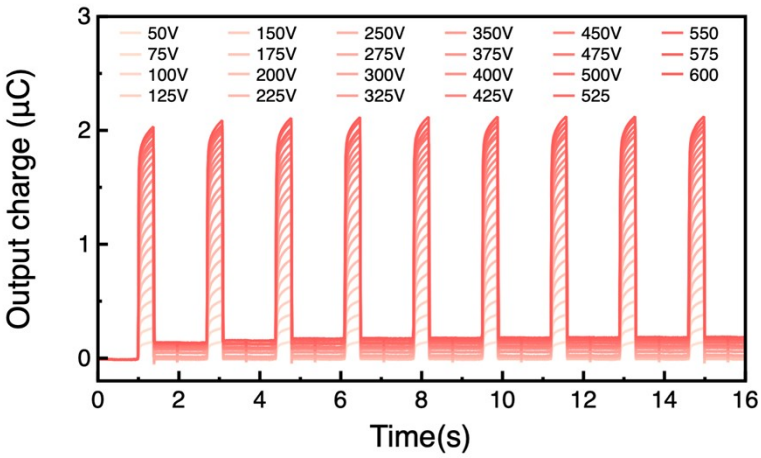

Figure S22. Short-circuit output charge curves of the charge-excitation generator under different applied voltages on C_{ce}.

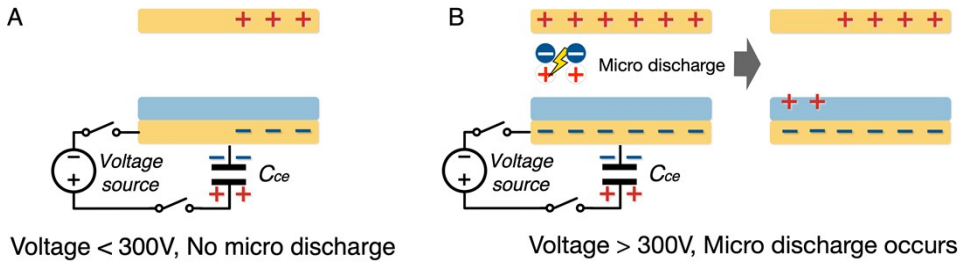

Figure S23. Schematic diagram of micro-discharge phenomenon induced by high applied voltage.

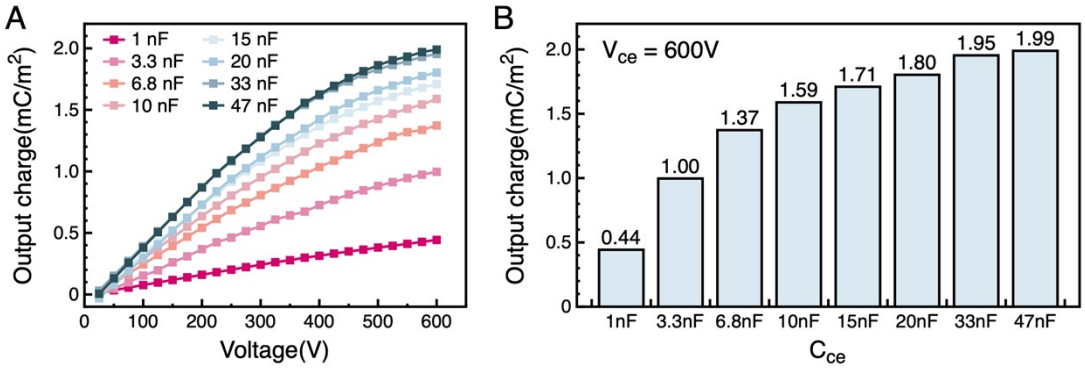

Figure S24. Output charge of the charge excitation generator with different C_{ce}.

(A) Output charge versus applied voltage on C_{ce} for various values of C_{ce}.

(B) Relationship between output charge and C_{ce} at V_{ce} = 600V.

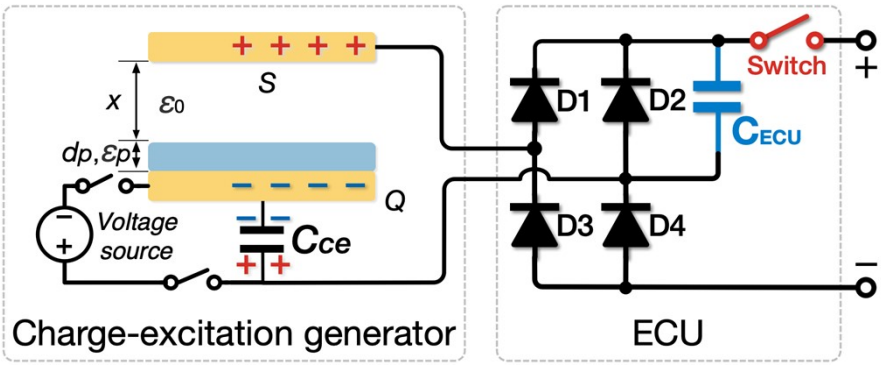

Figure S25. Schematic diagram of the connection between the charge excitation generator and the ECU featuring capacitor switching strategy

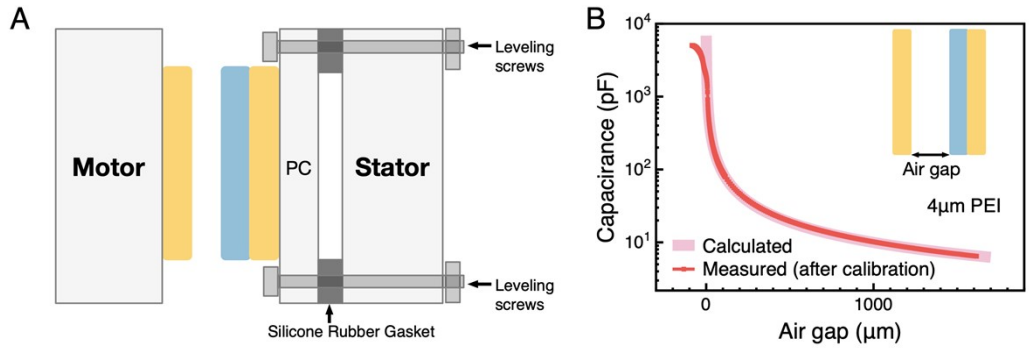

Figure S26. Alignment adjustment setup for the generator and its capacitance at different separation distances.

(A) Schematic diagram of the alignment adjustment setup for the generator, mounted on a linear motor.

(B) The capacitance of the generator at different distances after alignment calibration.

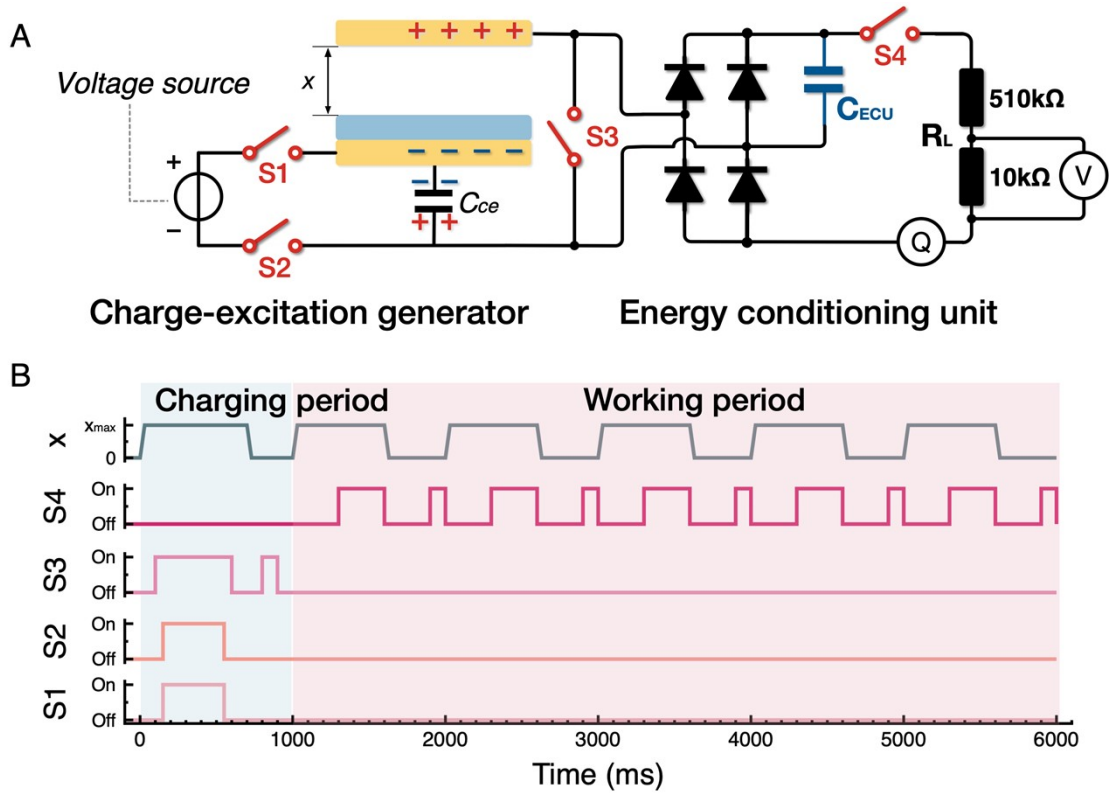

Figure S27. Experimental setup for measuring the maximum achievable output of the generator.

(A) Schematic diagram of the experimental setup.

(B) Timing chart illustrating the on-off states of the switches and the motion of the generator.

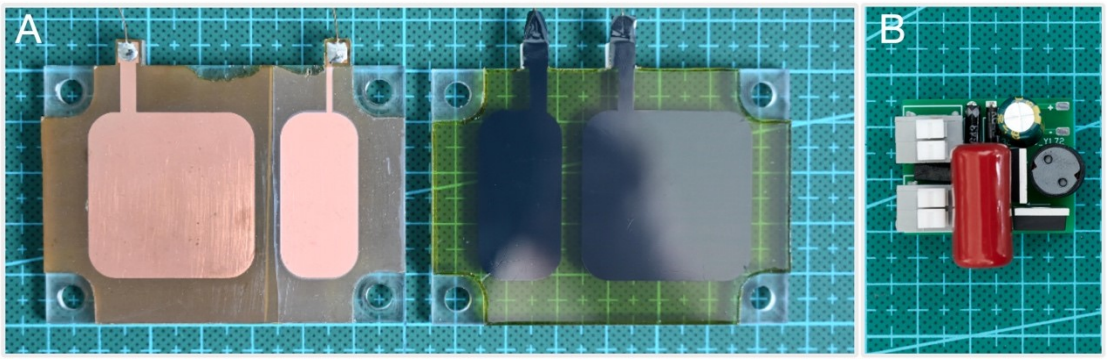

Figure S28. Image of the (A) fabricated generator, (B) ECU featuring capacitor-switching strategy, and LC passive buck converter.

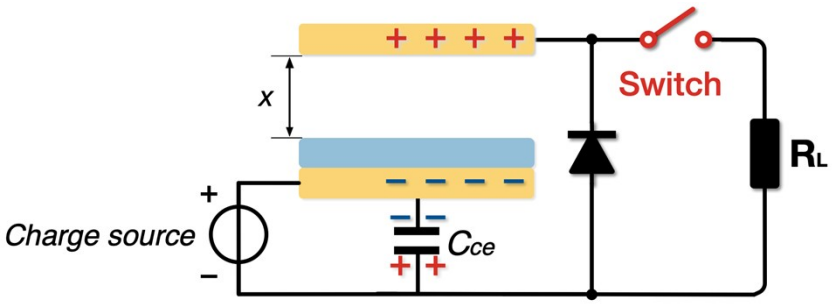

Figure S29. Simplified model of ECU #4, applicable when the maximum separation distance of the generator is less than the C_{ECU} transition distance.

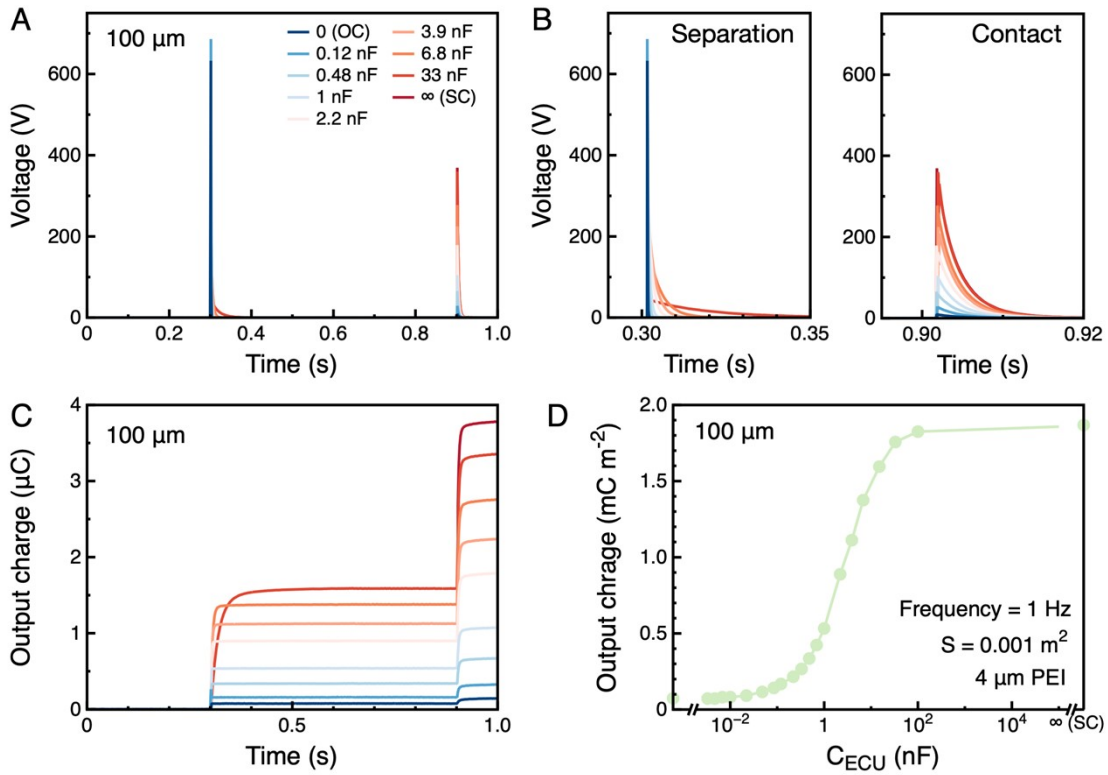

Figure S30. Maximum achievable output voltage and charge of the generator under the maximum separation distance of 100 μm.

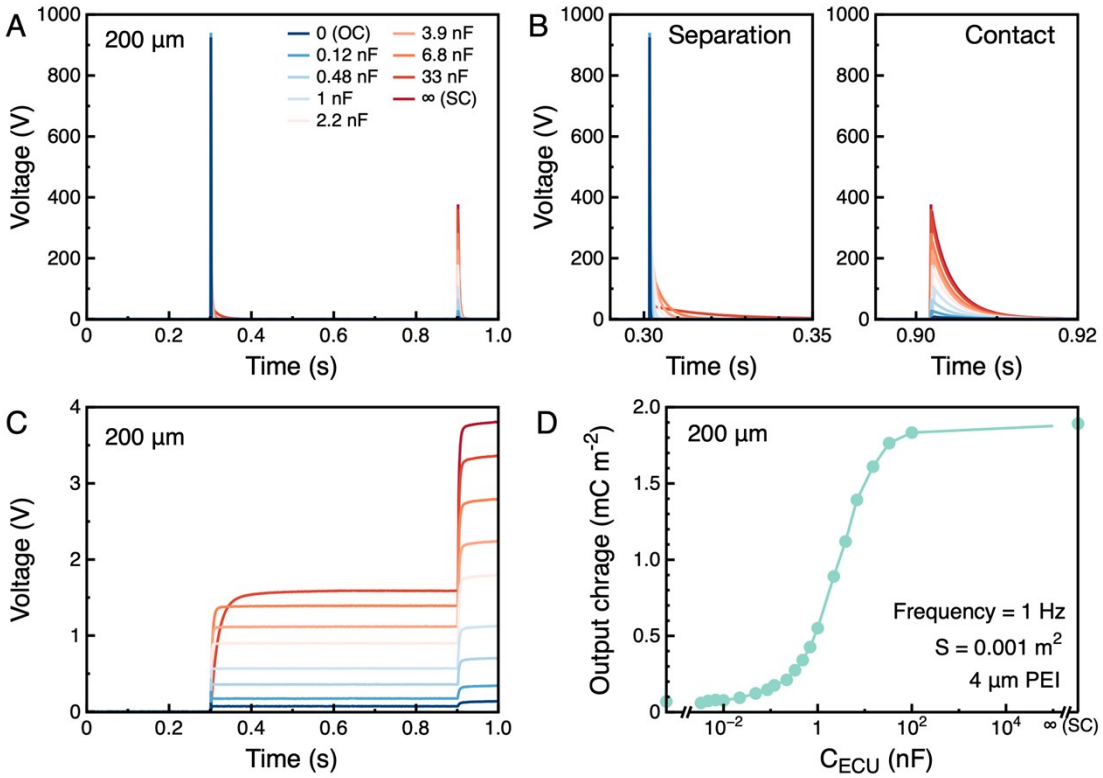

Figure S31. Maximum achievable output voltage and charge of the generator under the maximum separation distance of 200 μm.

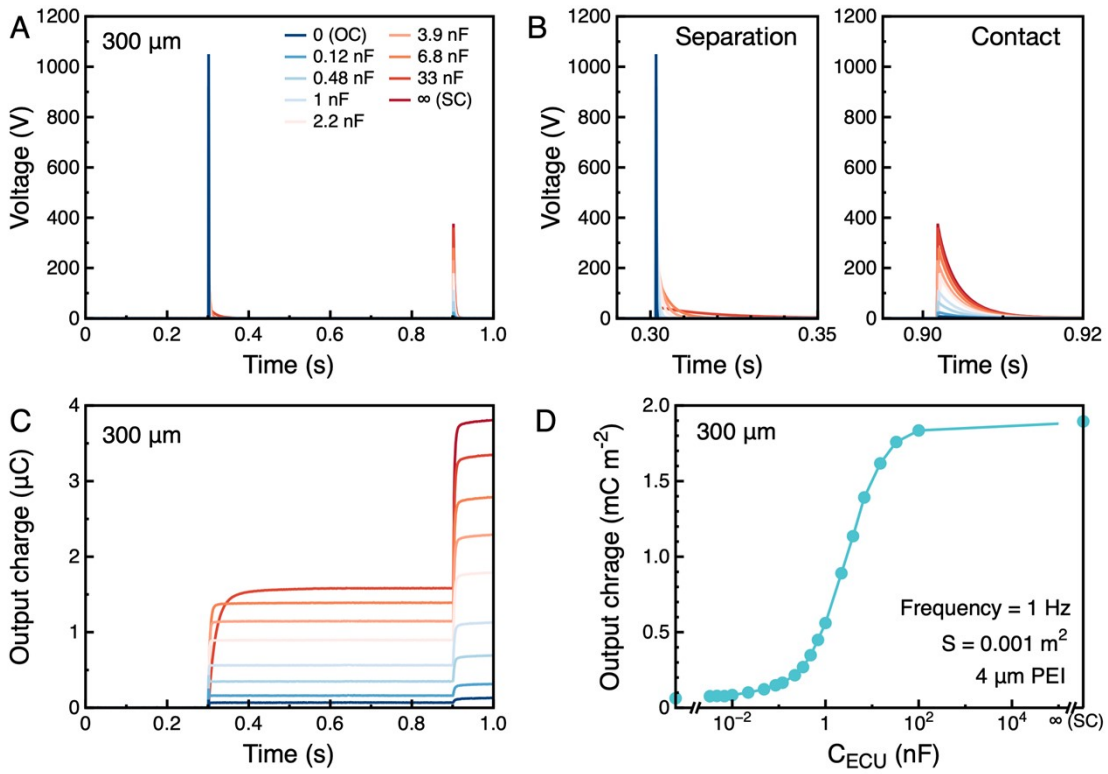

Figure S32. Maximum achievable output voltage and charge of the generator under the maximum separation distance of 300 μm.

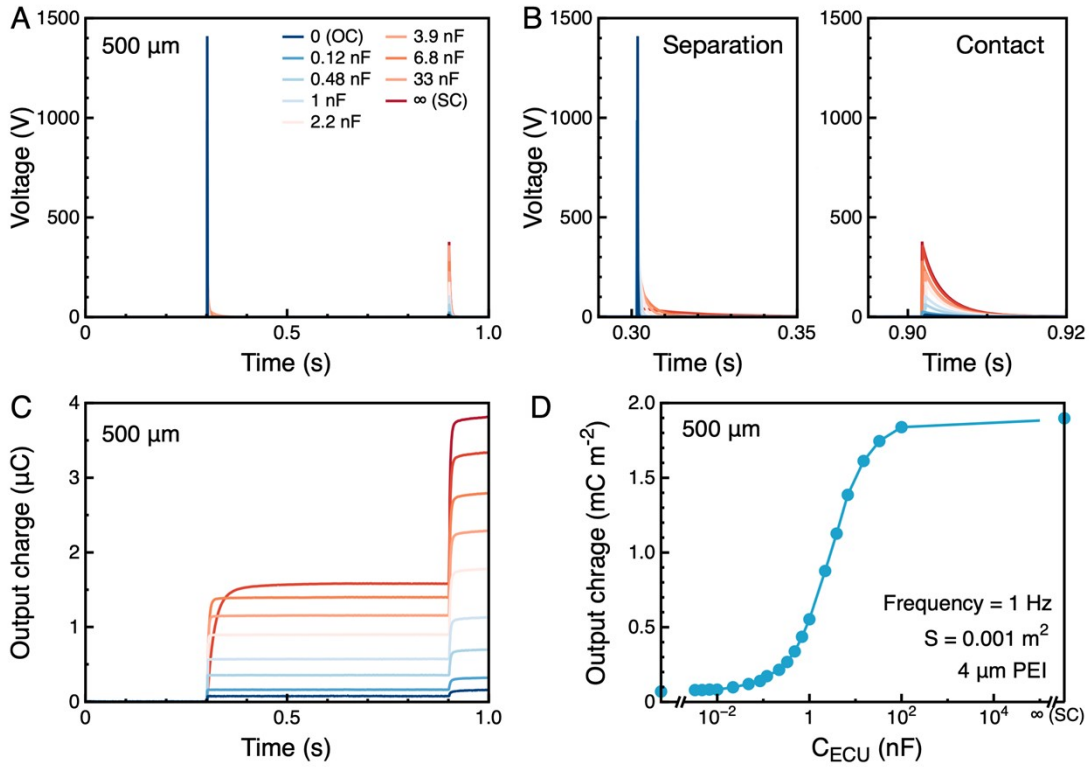

Figure S33. Maximum achievable output voltage and charge of the generator under the maximum separation distance of 500 μm.

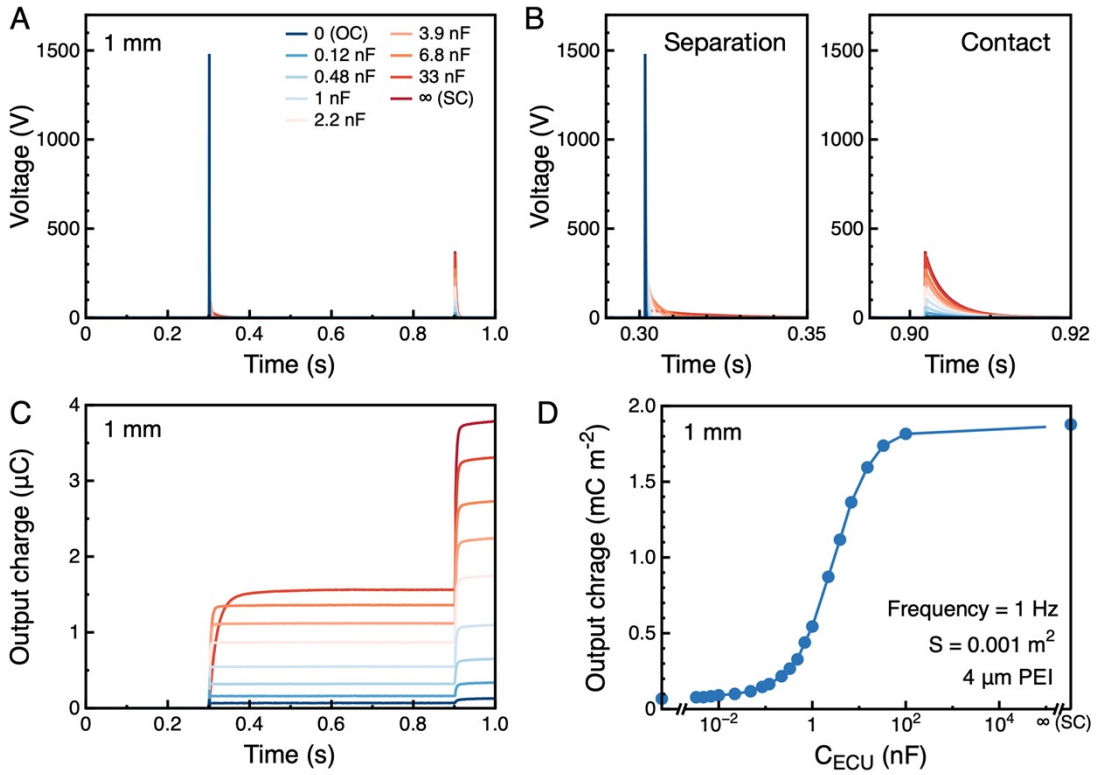

Figure S34. Maximum achievable output voltage and charge of the generator under the maximum separation distance of 1 mm.

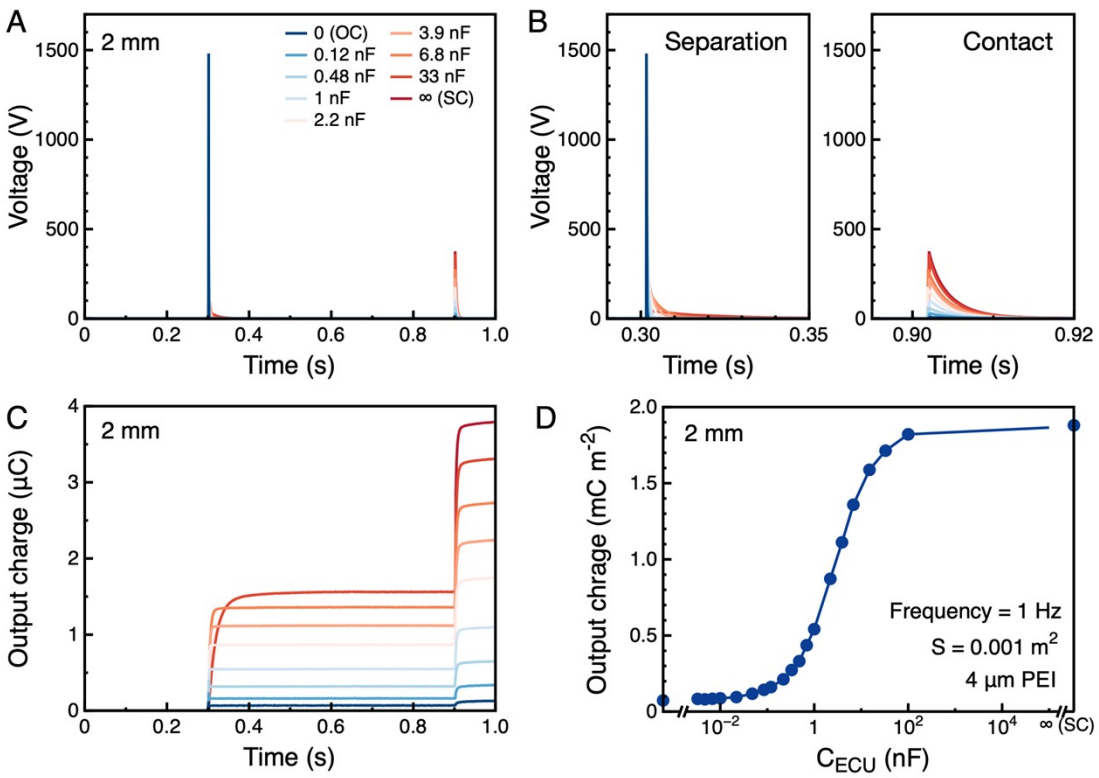

Figure S35. Maximum achievable output voltage and charge of the generator under the maximum separation distance of 2 mm.

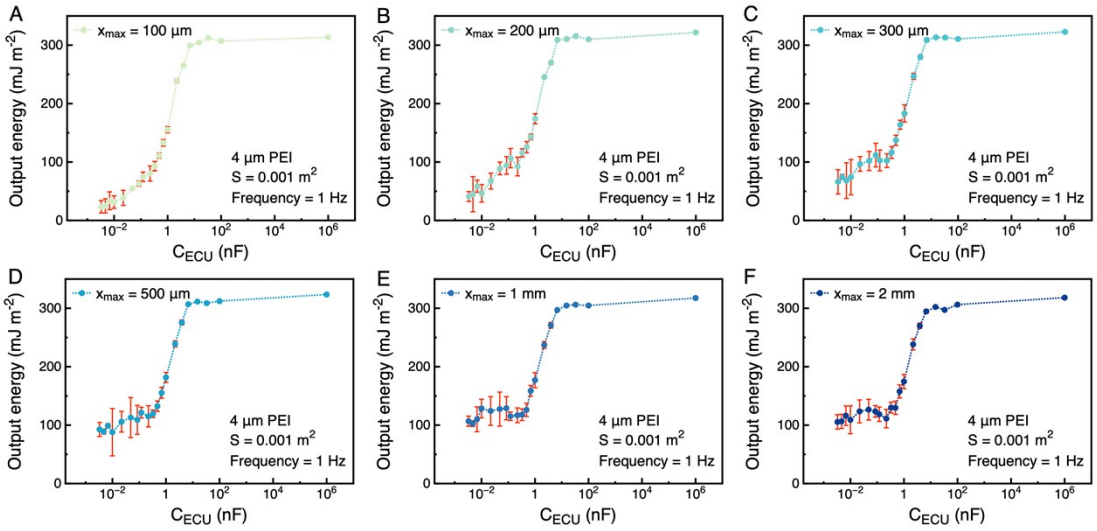

Figure S36. Comparison of the generator's maximum achievable output under different maximum separation distances.

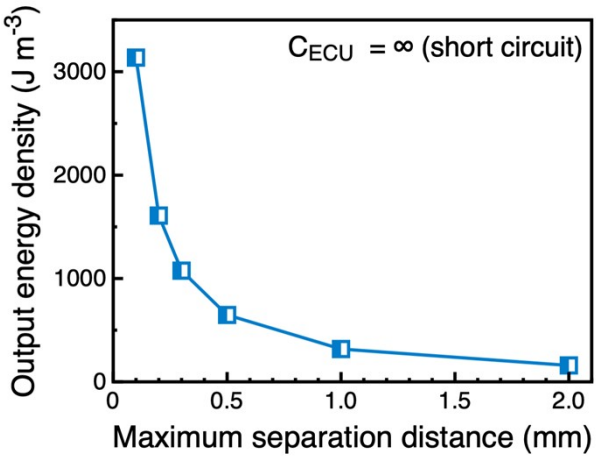

Figure S37. Volumetric energy density of the generator under different maximum separation distances.

Here, the volume for the calculation of volumetric energy density refers to the difference between the maximum expansion volume and the compression volume of the generator.

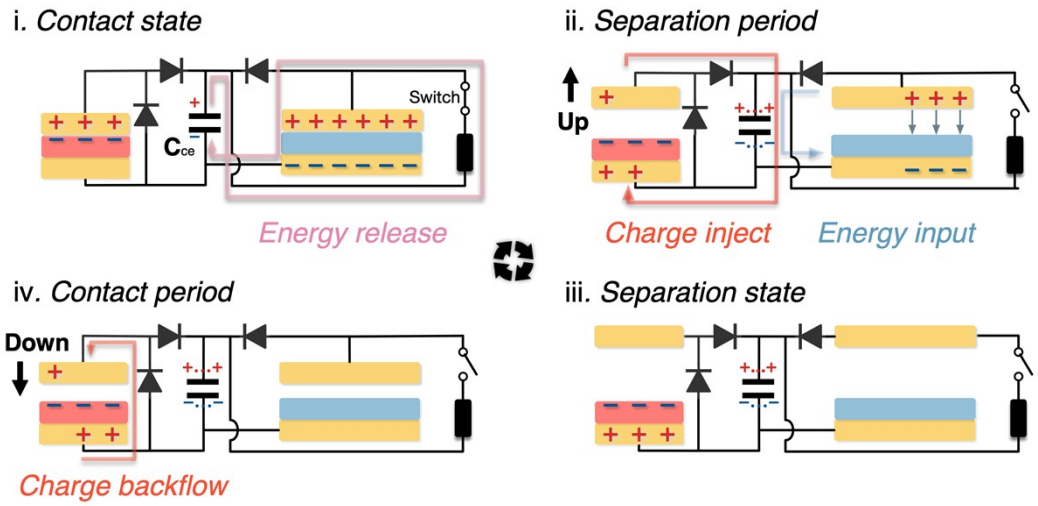

Figure S38. Working process of the charge-excitation generator through the external pump.

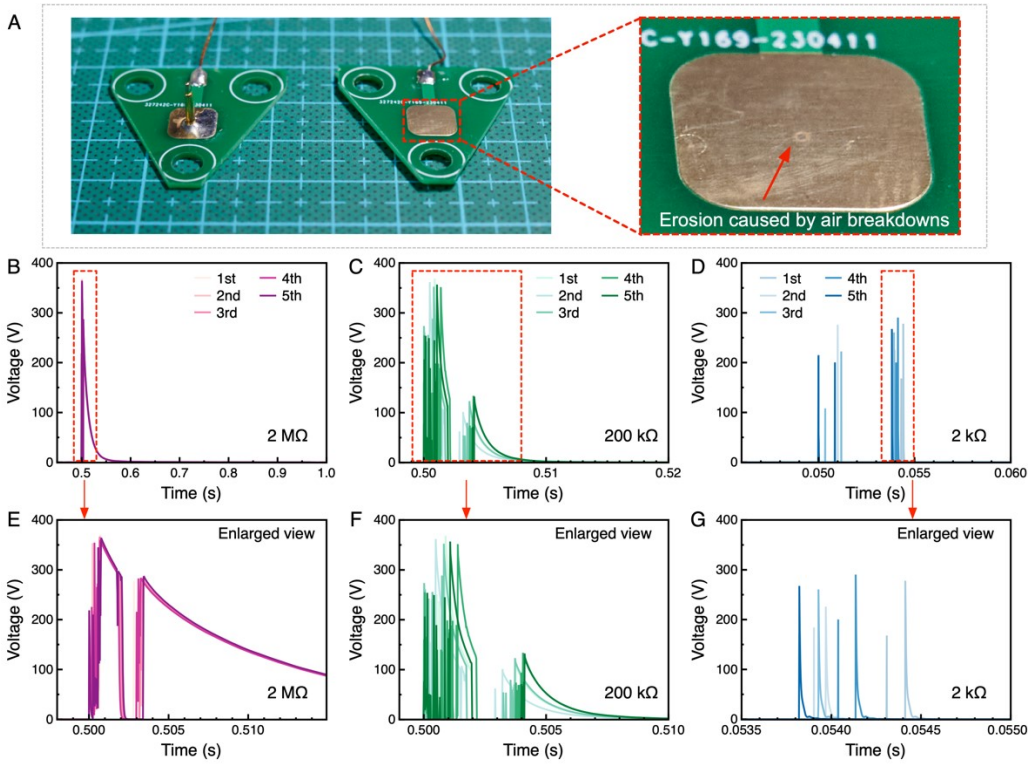

Figure S39. Output characteristics of the generator after the synchronous switch.

(A) Image of the contact switch with an enlarged view of the erosion trace due to random air breakdowns.

(B to G) Output voltage after the contact switch with the load resistances of 2MΩ, 200kΩ, and 2kΩ, respectively, along with their enlarged views.

Based on the voltage divider rule and output voltages on the load resistance, the contact resistance of the switch due to the erosion ranges from approximately 500 to 1000 Ω. Additionally, regardless of the load resistance value, random air breakdowns and mechanical bounces consistently occur within the first 5 ms of the closure time.

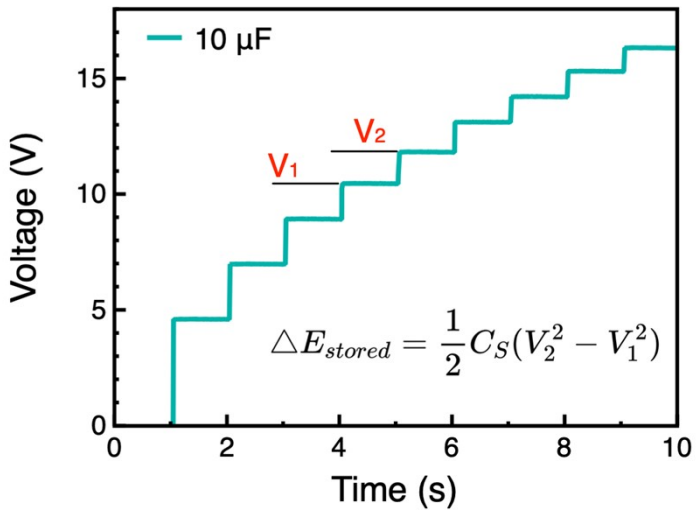

Figure S40. Calculation method for the stored energy in a single working cycle.

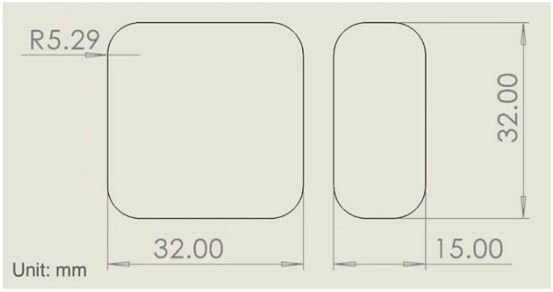

Figure S41. Dimensions of the electrodes of the charge-excitation generator.

Table S1. Comparison of performance of the electrostatic generators.

No	Electrode Size	Maximum separation distance	Pulse Output Energy	DC Output Power	Area density (Pulsed)	Area density (DC)	Volumetric density (Pulsed)	Volumetric density (DC)	Ref.
1	0.00325 m^2	5mm	25 μJ	9.0μW @ 1Hz	10.8mJ m^{-2}	2.8mW m^{-2} Hz^{-1}	2.16J m^{-3}	0.56 W m^{-3} Hz^{-1}	Xi et al. 2017[1]
2	0.0096 m^2	3mm	93.3 μJ	67.6μW @ 1Hz	9.7mJ m^{-2}	6.9mW m^{-2} Hz^{-1}	3.23J m^{-3}	2.3 W m^{-3} Hz^{-1}	Cheng et al. 2017[2]
3	0.0032 m^2	5mm	83.6 μJ	251.9μW @ 3.3Hz	26.1mJ m^{-2}	23.9mW m^{-2} Hz^{-1}	5.22J m^{-3}	4.78 W m^{-3} Hz^{-1}	Harmon et al. 2020[3]
4	0.002 m^2	9mm	138.8 μJ	30.07μW @ 3.3Hz	69.4mJ m^{-2}	37.09mW m^{-2} Hz^{-1}	7.71J m^{-3}	4.12 W m^{-3} Hz^{-1}	Liu et al. 2020[4]
5	0.001 m^2	2mm	130 μJ	92.7μW @ 1Hz	130mJ m^{-2}	92.7mW m^{-2} Hz^{-1}	65J m^{-3}	46.35 W m^{-3} Hz^{-1}	Gao et al. 2023[5]
6	0.01 m^2	9.6mm	1.4 mJ	110mW @ 1Hz	142mJ m^{-2}	110mW m^{-2} Hz^{-1}	14.79J m^{-3}	11.46 W m^{-3} Hz^{-1}	Wang et al. 2021[6]
7	0.00072 m^2	2mm	132.5 μJ	73.3 μW@ 1Hz	184 mJ m^{-2}	101.8 mW m^{-2} Hz^{-1}	92 J m^{-3}	50.9 W m^{-3} Hz^{-1}	Guo et al. 2023[7]
8	**0.001 m^2**	**100μm**	**289 μJ**	**152μW@ 1Hz**	**289mJ m^{-2}**	**152mW m^{-2} Hz^{-1}**	**2890J m^{-3}**	**1520 W m^{-3} Hz^{-1}**	**This work**

Note. The calculation method of volumetric energy density refers to the difference between the maximum expansion volume and the compression volume of the main generator, where the electrode size is 0.001m^2, and the maximum separation distance is 100 μm.

Table S2. The default parameters of the generator.

Parameters			**Value**
Mechanical		Effective dielectric thickness (d_r/ε_r)	10 μm
		Area Size (A)	0.001 m^2
		Maximum separation distance (x_{max})	100 μm
		Operation frequency (*f*)	1 Hz
Electrical	ECU #1	Maximum retainable charge density (σ_m)	294.44 μC m^{-2}
		Optimal load (R_{opt})	100.873 MΩ
	ECU #2	Maximum retainable charge density (σ_m)	74.93 μC m^{-2}
		Load resistance	0.1Ω
	ECU #3	Maximum retainable charge density (σ_m)	208.04μC m^{-2}
		Optimal external capacitance ($C_{ECU\text{-}opt}$)	316.74 pF
		Load resistance	0.1Ω

Note S1

A simple proof that the input and output energy of an electrostatic generator are equal in steady state.

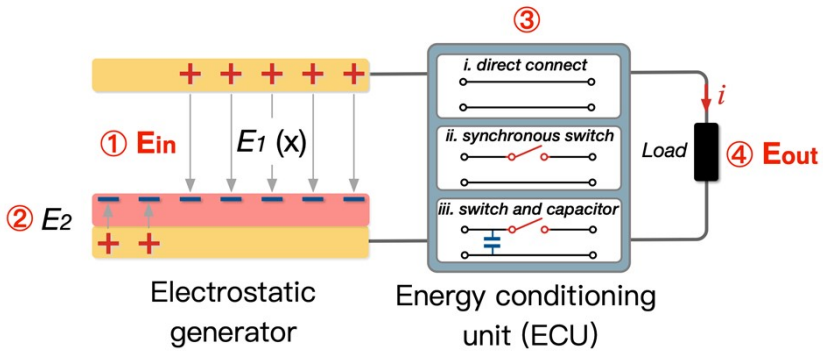

Figure S42. Schematic diagram and the energy conversion process of electrostatic generator system.

The schematic diagram and energy conversion process of the electrostatic generator system is shown in Figure S42. Within one working cycle, the mechanical energy input into the generator equals the work done by the charges on the moving upper electrode against the electric field force (①), represented by the area of the $\frac{1}{2}\varepsilon_0 E(x)^2 - x$ plot. Part of this input energy is stored in the energy storage components of the system, such as the capacitor of the dielectric film of the generator (②) or the capacitors within the energy conditioning unit (③); while other portions is consumed by the load (④) or dissipated through wires and other components (③). The input energy within one working cycle satisfies the following equation:

$$E_{in} = \Delta E_{store} + E_{diss} + E_{out}$$

where E_{in} is the energy input into the generator, $\triangle E_{\text{store}}$ is the energy stored in the system, E_{diss} is the dissipated energy, and E_{out} is the energy obtained by the load.

Generally, the operation of the generator goes through two states: transient state and steady state. In transient state, the energy stored in the system varies with the working cycles, and $\triangle E_{\text{store}} \neq 0$. In this case, the energy input into the generator does not equal

to the energy consumed by the system, and the maximum amplitude of the output voltage in this state varies among each cycle. Then, when the system goes into the steady state, the stored energy in the system is saturated and reaches stable, and $\triangle E_{\text{store}} = 0$. Thus, the energy input into the generator system equals its energy output, and the output voltage becomes periodic and stable. Generally, the energy dissipation in the circuit is much smaller than the energy obtained by the load. Thus, if we neglect the energy dissipation in the circuit, the energy input to the generator and the output to the load are equal in the steady state.

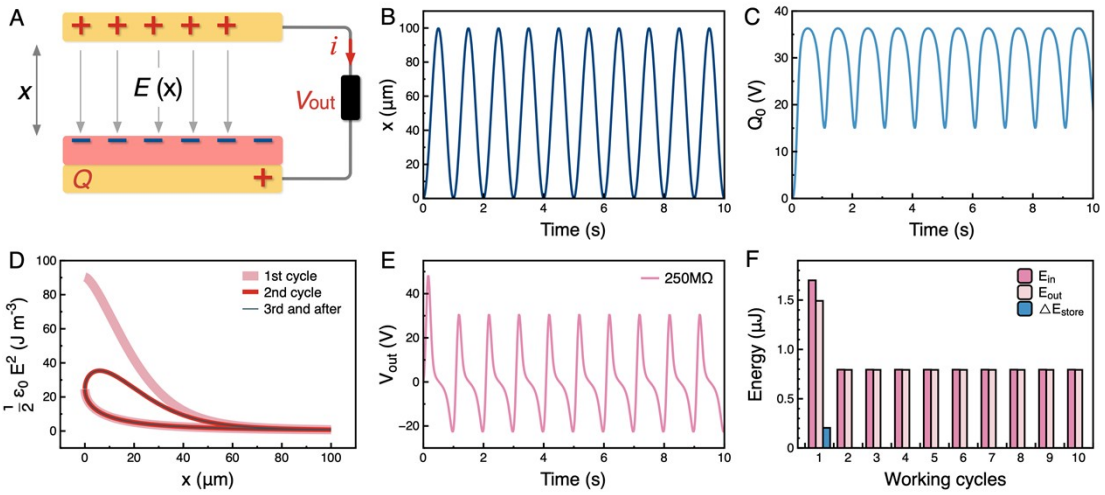

Figure S43. The energy transfers in a conventional generator within 10 working cycles. (Surface charge density = -40 μC m^{-2}, electrode size = 0.001 m^2, effective thickness of dielectric = 10 μm, maximum separation = 100 μm, load resistance = 250 MΩ, frequency = 1 Hz, sinusoidal stimulation).

(A) Schematic of a generator that directly connected with a load resistance.

(B to E) The separation distance, transferred charge, $\frac{1}{2}\varepsilon_0 E(x)^2 - x$ plot, and output voltage of the generator, respectively.

(F) The input energy, output energy, and stored energy of the generator in a single working cycle.

Taking a conventional generator as an example, the $\frac{1}{2}\varepsilon_0 E(x)^2 - x$ plot, output voltage, the

charge on the lower electrode, input energy, output energy, and the energy stored in the capacitor of the dielectric film are calculated and shown in Figure S43. The initial conditions of the calculation are set to be x = 0 (t = 0), Q = 0 (t = 0), and dQ/dt = 0 (t = 0), and the upper electrode is driven by the sinusoidal excitation (Figure S43B). It can be found that in the first working cycle, the generator is in the transient state. In this state, the input energy is larger than the output energy, and the energy stored in the capacitor of the dielectric film $\triangle E_{\text{store}}$ is larger than 0, thus the output voltage is not stable. Then, with the increase of the generator working cycle, the energy stored in the generator's storage unit gradually tends to stabilize, the energy deposited into the storage unit in a single cycle $\triangle E_{\text{store}}$ tends to 0, and the generator reaches the steady state. Thus, the output voltage becomes stable and periodic, and the generator input energy and the output energy are equal.

Note S2

The calculation procedure of the maximum achievable output energy of the generator with different ECUs under air breakdown limitation.

S2.1 Calculation procedure for maximum achievable output of the generator with ECU #1

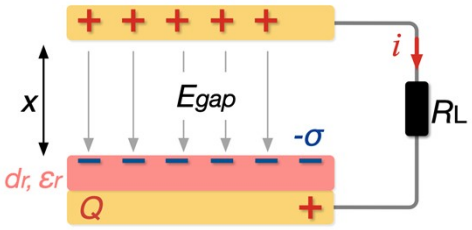

Figure S44. Schematic of the generator with ECU #1.

Step 1: *Calculating the maximum retainable charge density (σ_m) of the generator at steady state under air breakdown limitations.*

The governing equation of the generator is:

$$\frac{\sigma_{init}}{\varepsilon_0}x-\frac{Q}{S\varepsilon_0}\left(x+\frac{d_r}{\varepsilon_0}\right)=\frac{dQ}{dt}R_L \tag{S1}$$

Given an initial charge density on the dielectric σ_{init}, the motion of the upper electrode of the generator x and the load resistance R_L, the output charge Q of the generator, namely, the charge on the lower electrode, in steady state can be easily obtained. Then, the electric field strength of the generator in the air gap during the separation process ($x = 0 \rightarrow x_{max}$) can be obtained with the obtained Q, as shown below:

$$E_{gap}(x)=\frac{\sigma_{init}-\frac{Q}{S}}{\varepsilon_0} \tag{S2}$$

Then, the minimum ratio between the field strength of the generator and the air breakdown threshold can be obtained as:

$$r_{min}=\min\left(\frac{E_b(x)}{E_{gap}(x)}\right), x\in[0,x_{max}] \tag{S3}$$

where E_b is defined by Paschen's Law (Equation 3). Then, the maximum charge density

that can be retained by the generator can be calculated as:

$$\sigma_m = r_{min} \times \sigma_{init} \tag{S4}$$

Step 2: *Calculating the maximum achievable output of the generator with air breakdown limitations*.

Using σ_m to replace σ_{init} in Equation (S1), the maximum achievable output voltage, output charge, $\frac{1}{2}\varepsilon_0 E(x)^2 - x$ plot, and output energy of the generator with the load of R_L in the steady state can be obtained. By iteratively calculating the maximum achievable output of the generator under all loads, the maximum achievable output of the generator under the air breakdown limit with this ECU can be obtained.

S2.2 Calculation procedure for maximum achievable output of the generator with ECU #2 and ECU #3

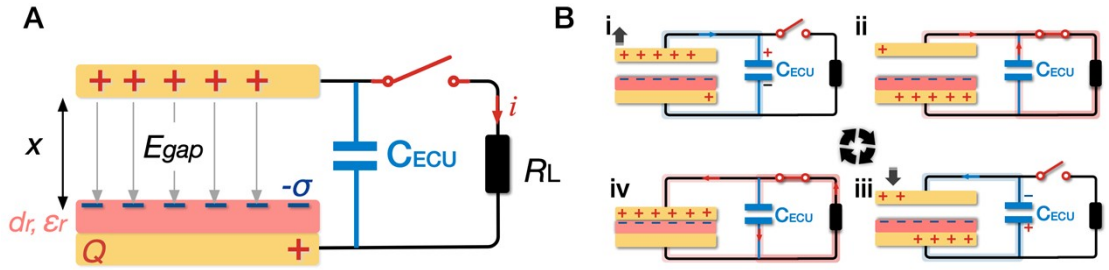

Figure S45. (A)Schematic and (B) working process of the generator with ECU #3.

The schematic diagram of the generator with ECU #3 and its working principle in a single working cycle is shown in Figure S45. The external capacitor is connected with the generator in parallel, and the synchronous switch opens during the separation and contact processes and closes at the maximum separation state and contact state. For simplicity, the load resistance here is considered to be sufficiently small, and the energy in the generator and external capacitor can be fully transferred to the load during the closure time of the switch. The calculation procedure of the output of the generator with ECU #3 is shown below. As ECU #2 can be regarded as ECU #3 with $C_{ECU} = 0$, the following calculation procedure also can be used to calculate the output of the generator with ECU #2.

Step 1: *Calculating the maximum retainable charge density (σ_m) of the generator under air breakdown limitations.*

In the separation period (Figure S45 Bi), the switch opens, and the generator is connected with C_{ECU} in parallel. As the separation distance increases, the charge from the upper electrode flows into C_{ECU}. The electric field strength of the air gap during this period is：

$$E_{gap}(x) = \frac{\sigma}{\varepsilon_0} \times \frac{\frac{d_r}{\varepsilon_r} + \frac{\varepsilon_0 S}{C_{ECU}}}{\frac{d_r}{\varepsilon_r} + \frac{\varepsilon_0 S}{C_{ECU}} + x} \tag{S5}$$

To avoid air breakdown, E_{gap} must be less than the air breakdown threshold E_{b}. Therefore, the maximum charge density that can be retained by the generator can be calculated as:

$$\sigma_m = \min\left(\frac{\frac{d_r}{\varepsilon_r} + \frac{\varepsilon_0 S}{C_{ECU}} + x}{\frac{d_r}{\varepsilon_r} + \frac{\varepsilon_0 S}{C_{ECU}}} \times \varepsilon_0 E_b(x) \right), x \in [0, x_{max}] \tag{S6}$$

Step 2: *Calculating the maximum achievable output of the generator*.

In the initial state, the contact state (Figure S45 Biv), the charge on the dielectric surface is balanced by the charge on the upper electrode. Then, the upper electrode moves upward (Figure S45 Bi), the electric field strength of the air gap in the separation period can be calculated as:

$$E_{sep} = \frac{\sigma_m}{\varepsilon_0} \times \frac{\frac{d_r}{\varepsilon_r} + \frac{\varepsilon_0 S}{C_{ECU}}}{\frac{d_r}{\varepsilon_r} + \frac{\varepsilon_0 S}{C_{ECU}} + x} \tag{S7}$$

When the upper electrode of the generator reaches the maximum separation position (Figure S45 Bii), the switch closes and the output voltage on the load is：

$$V_{out-sep} = \frac{S\sigma_m \quad x_{max}}{C_{ECU}\frac{d_r}{\varepsilon_r} + \frac{\varepsilon_0 S}{C_{ECU}} + x_{max}} \times e^{-\frac{t}{R_L(C_{ECU} + \frac{\varepsilon_0 S}{x_{max} + \frac{d_r}{\varepsilon_r}})}} \tag{S8}$$

Assuming that the load resistance is small enough, the output charge of the generator during the closure time of the switch is:

$$Q_{out} = S\sigma_m \times \frac{x_{max}}{x_{max} + \frac{d_r}{\varepsilon_r}} \tag{S9}$$

Then, the switch opens, and the upper electrode moves downward (Figure S45 Biii). The electric field strength of the air gap during this period is:

$$E_{con} = \left(\frac{\sigma_m d_r}{\varepsilon_0\, \varepsilon_r} + \frac{S\sigma_m - Q_{out}}{C_{ECU}}\right)\frac{x}{\varepsilon_0 S} / \left(\frac{d_r}{\varepsilon_r \varepsilon_0 S} + \frac{x}{\varepsilon_0 S} + C_{ECU}\right) \tag{S10}$$

When the generator reaches the contact state (Figure S45 Biv), the switch closes and the output voltage on the load is：

$$V_{out-con} = \frac{Q_{out}}{S\varepsilon_0} \times \frac{d_0}{C_{ECU} + \frac{\varepsilon_r \varepsilon_0 S}{d_r}} e^{-\frac{t}{R_L(C_{ECU} + \frac{\varepsilon_r \varepsilon_0 S}{dr})}} \tag{S11}$$

Then, the maximum output of the generator can be calculated by the $\frac{1}{2}\varepsilon_0 E(x)^2 - x$ plot based on Equation (S7) and (S10). For ECU #3, the key factor affecting the output performance is the value of C_{ECU}. By iteratively calculating the maximum output of the generator under all C_{ECU} values, the maximum achievable output of the generator under the air breakdown limit with this ECU can be obtained.

S2.3 Calculation procedure for ECU #4 ——capacitor-switching.

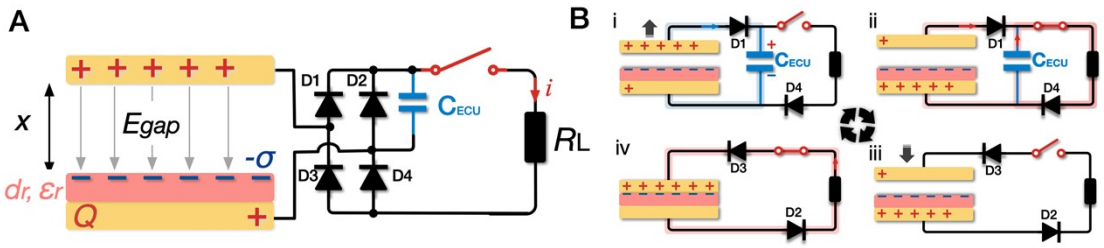

Figure S46. (A)Schematic and (B) working process of the generator with ECU #4.

The working process of the generator with ECU #4 is similar to that with ECU #3, as shown in Figure S46. The only difference between them is the connection of C_{ECU}. For ECU #4, C_{ECU} is connected in parallel with the generator during the separation period but is shielded during the contact period. In contrast, for ECU #3, the C_{ECU} remains connected in parallel with the generator throughout the entire cycle. For simplicity, we also assume that the load resistance is sufficiently low, meaning that the generator's output energy can be fully transferred to the load during the brief closure time of the switch. In calculation, the diodes and the switch are treated as ideal ones. The procedure for calculating the maximum achievable output of the generator under air breakdown limitations is as follows:

Step 1: *Calculating the maximum retainable charge density (σ_m) of the generator under air breakdown limitations.*

During the separation period (Figure S46 Bii), the switch is open, and the generator is connected in parallel with C_{ECU}, which is the same as the configuration for the generator with ECU #3. Consequently, the equation for calculating the maximum charge density that can be retained by the generator is the same as that used for ECU #3, as shown below:

$$\sigma_m = \min\left(\frac{\frac{d_r}{\varepsilon_r}+\frac{\varepsilon_0 S}{C_{ECU}}+x}{\frac{d_r}{\varepsilon_r}+\frac{\varepsilon_0 S}{C_{ECU}}}\times \varepsilon_0 E_b\right), x\in[0,x_{max}] \tag{S12}$$

Step 2: *Calculating the maximum achievable output of the generator*.

In the initial state, the contact state (Figure S46 Biv), the charge on the dielectric surface is balanced by the charge on the upper electrode. Then, the upper electrode moves upward (Figure S46 Bi), the electric field strength of the air gap in the separation period is:

$$E_{sep} = \frac{\sigma_m}{\varepsilon_0} \times \frac{\frac{d_r}{\varepsilon_r} + \frac{\varepsilon_0 S}{C_{ECU}}}{\frac{d_r}{\varepsilon_r} + \frac{\varepsilon_0 S}{C_{ECU}} + x} \tag{S13}$$

When the upper electrode of the generator reaches the maximum separation position (Figure S46 Bii), the switch closes and the output voltage on the load is：

$$V_{out-sep} = \frac{S\sigma_m \quad x_{max}}{C_{ECU}\frac{d_r}{\varepsilon_r} + \frac{\varepsilon_0 S}{C_{ECU}} + x_{max}} \times e^{-\frac{t}{R_L(C_{ECU} + \frac{\varepsilon_0 S}{x_{max} + \frac{d_r}{\varepsilon_r}})}} \tag{S14}$$

Assuming that the load resistance is small enough, the output charge of the generator during the closure time of the switch is:

$$Q_{out} = S\sigma_m \times \frac{x_{max}}{x_{max} + \frac{d_r}{\varepsilon_r}} \tag{S15}$$

Then, the switch opens, C_{ECU} is shielded, and the upper electrode moves downward (Figure S46 Biii). The electric field strength of the air gap during this period is:

$$E_{con} = \frac{\sigma_m}{\varepsilon_0} - \frac{Q_{out}}{S\varepsilon_0} \tag{S16}$$

When the generator reaches the contact state (Figure S46 Biv), the switch closes and the output voltage on the load is：

$$V_{out-con} = Q_{out}\frac{d_0}{S\varepsilon_0} \times e^{-\frac{t}{R_L(\frac{\varepsilon_0 S}{d0})}} \tag{S17}$$

Then, the maximum output of the generator can be calculated by the $\frac{1}{2}\varepsilon_0 E(x)^2 - x$ plot based on Equation (S13) 13 and (S16). For ECU #4, the key factor affecting its output performance is also the value of C_{ECU}. By iteratively calculating the maximum output of the generator under all C_{ECU} values, the maximum achievable output of the generator under the air breakdown limit with this ECU can be obtained.

It should be noted that the fundamental reason for the enhancement in the

generator's output achieved by ECU #4 is that it combines the benefits of ECU #2 and ECU #3. During the separation period, ECU #4 utilizes the external capacitor to regulate the variation of E_{gap} with separation distance, similar to ECU #3, which brings E_{gap} in the separation period closer to the breakdown threshold. Conversely, during the contact period, ECU #4 shields the external capacitor to ensure that E_{gap} remains constant and nearly 0, similar to ECU #2. Finally, the area of the $\frac{1}{2}\varepsilon_0 E(x)^2 - x$ plot is expanded, and the output of the generator is enhanced.

Note S3

The proof of equivalence between charge excitation generators and conventional generators

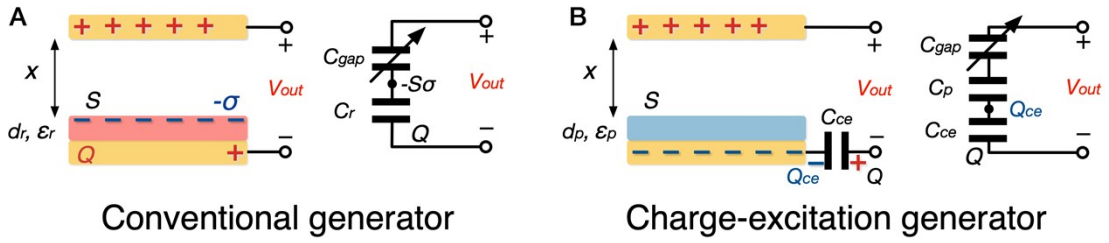

Figure S47. Schematic diagram and the Lumped circuit model of the conventional generator and the charge excitation generator.

The schematic diagrams and equivalent lumped circuit models of the conventional generator and the pump generator are illustrated in Figure S47.

1) For the conventional generator, its output voltage is given by：

$$V_{out} = \frac{S\sigma}{C_{gap}} - Q\left(\frac{1}{C_r} + \frac{1}{C_{gap}}\right) \tag{S18}$$

where σ is the charge density on the dielectric, S is the area size of the electrode, Q is the output charge of the generator, namely, the charge on the lower electrode for this generator; C_{gap} and C_r are the equivalent capacitances of the air gap and dielectric film, respectively.

2) For the charge-excitation generator, its output voltage is given by：

$$V_{out} = \frac{Q_{ce}}{C_{gap}} + \frac{S\sigma}{C_p} - Q\left(\frac{1}{C_{ce}} + \frac{1}{C_p} + \frac{1}{C_{gap}}\right) \tag{S19}$$

Where C_{ce} is the charge storage capacitor, Q_{ce} is the charge injected into C_{ce} from an external charge source, C_{gap} and C_p are the equivalent capacitances of the air gap and the insulating film, respectively. Q is the output charge of the generator. Here, defining $q = Q - Q_0$, where Q_0 denotes the charge on the generator's lower electrode in the contact state and is given by

$$Q_0 = Q_{ce}\frac{C_{ce}}{C_{ce}+C_p} \tag{S20}$$

Taking the expression of $Q = q + Q_0$ into Equation (S19), we can obtain:

$$V_{out} = Q_{ce}\frac{C_p \quad 1}{C_{ce}+C_pC_{gap}} + q\left(\frac{1}{C_{ce}}+\frac{1}{C_p}+\frac{1}{C_{gap}}\right) \tag{S21}$$

By setting

$$\begin{cases} \#\#\sigma_0 = \dfrac{Q_{ce} \quad C_p}{S \;\; C_{ce}+C_p} \\ \#C_{r0} = \dfrac{C_{ce}\times C_p}{C_{ce}+C_p} \end{cases} \tag{S22}$$

The Equation (S21) can be further simplified to:

$$V_{out} = \frac{S\sigma_0}{C_{gap}} - q\left(\frac{1}{C_{r0}}+\frac{1}{C_{gap}}\right) \tag{S23}$$

whose form is identical to Equation (S18). Therefore, the output of the Charge Excitation generator can be entirely equivalent to that of a conventional generator through Equation (S22). Furthermore, neglecting edge effects and setting

$$C_{r0} = \frac{S\varepsilon_0}{d_0} \tag{S24}$$

Equation (S22) can be further simplified to:

$$\begin{cases} \#d_0 = \dfrac{d_p}{\varepsilon_p} + \dfrac{S\varepsilon_0}{C_{ce}} \\ \#\sigma_0 = \dfrac{Q_{ce} \quad 1}{S \quad 1+\dfrac{C_{ce}d_p}{S\varepsilon_0\varepsilon_p}} \end{cases} \tag{S25}$$

where d_0 is the effective thickness of the equivalent dielectric of the generator, and σ_0 is the equivalent charge density on the dielectric.

Supplemental References

1. Xi, F., Pang, Y., Li, W., Jiang, T., Zhang, L., Guo, T., Liu, G., Zhang, C., and Wang, Z.L. (2017). Universal power management strategy for triboelectric nanogenerator. Nano Energy 37, 168–176. 10.1016/j.nanoen.2017.05.027.

2. Cheng, X., Miao, L., Song, Y., Su, Z., Chen, H., Chen, X., Zhang, J., and Zhang, H. (2017). High efficiency power management and charge boosting strategy for a triboelectric nanogenerator. Nano Energy 38, 438–446. 10.1016/j.nanoen.2017.05.063.

3. Harmon, W., Bamgboje, D., Guo, H., Hu, T., and Wang, Z.L. (2020). Self-driven power management system for triboelectric nanogenerators. Nano Energy 71, 104642. 10.1016/j.nanoen.2020.104642.

4. Liu, W., Wang, Z., Wang, G., Zeng, Q., He, W., Liu, L., Wang, X., Xi, Y., Guo, H., Hu, C., et al. (2020). Switched-capacitor-convertors based on fractal design for output power management of triboelectric nanogenerator. Nat Commun 11, 1883. 10.1038/s41467-020-15373-y.

5. Gao, Y., Liu, D., Li, Y., Liu, J., Zhou, L., Li, X., Zhao, Z., Li, S., Yang, P., Wang, Z.L., et al. (2023). Achieving high-efficiency triboelectric nanogenerators by suppressing the electrostatic breakdown effect. Energy Environ. Sci. 16, 2304–2315. 10.1039/D3EE00220A.

6. Wang, Z., Liu, W., He, W., Guo, H., Long, L., Xi, Y., Wang, X., Liu, A., and Hu, C. (2021). Ultrahigh Electricity Generation from Low-Frequency Mechanical Energy by Efficient Energy Management. Joule 5, 441–455. 10.1016/j.joule.2020.12.023.

7. Guo, Z., Yang, P., Zhao, Z., Gao, Y., Zhang, J., Zhou, L., Wang, J., and Wang, Z.L. (2023). Achieving a highly efficient triboelectric nanogenerator via a charge reversion process. Energy Environ. Sci. 16, 5294–5304. 10.1039/D3EE02614K.